Complex Propagators in Perturbation Theory*

I. J. R. AITCHISON†
Brookhaven National Laboratory, Upton, New York

AND

C. KACSER‡
Columbia University, New York, New York

(Received 7 October 1963)

A method is given for studying the analytic properties of an arbitrary Feynman graph F, in which a full two-particle propagator G is inserted between one pair of points. Three special graphs are treated in detail: the two-particle amplitude itself, with two- and three-particle intermediate states, and the "triangle" graph. When G has a resonance, a possible approximation for F is to replace G by a complex pole, obtaining thereby a new graph f in which one internal particle has a complex mass. We show that, although the singularities of F and f are in general different, this approximation is appropriate for calculating "enhancement" effects due to singularities of F, near the physical region, associated with the resonance. For the cases considered, we predict the ranges of the external variables for which such effects will occur, and show how to calculate them explicitly.

1. INTRODUCTION

THE conventional analysis of perturbation theory graphs deals with those graphs which have stable intermediate states—corresponding to the "elementary" fields of the Lagrangian—as internal lines. However, it may well be, especially in view of the wealth of experimental examples, that one or more pairs of the elementary particles involved may interact to form resonant states; these states contain, in a certain energy range, the most important features of the appropriate two-particle system. If we regard these two-particle resonances as approximately stable, we are naturally led to ask how we may extend the usual analysis to include resonances as internal lines. If we could do this, it would correspond to selecting out the physically most important parts of the sum of all those graphs (involving only stable intermediate states) which contain as subgraphs all possible graphs in the appropriate two-particle propagator, but which are otherwise identical to each other.

This type of reduction of three-particle intermediate states has already been discussed from a rather different viewpoint by Mandelstam *et al.*,[1] by Zwanziger,[2] and Hwa.[3] These authors use equations derived from unitarity to analyze effects due to the coupling between elastic and inelastic channels when there is a resonance in one elastic channel. However, it is not evident how this work may be extended if the resonance occurs in a *crossed* channel. Our method is able to handle such cases, and it also recovers the results obtained by the unitarity method.

A third approach, related to both of these, has recently been investigated by G. Bonnevay.[4] It is based essentially on a model dispersion theory, the starting point being a Khuri-Treiman equation. Where they overlap, our results agree with those of Bonnevay.

The problem is formulated in Sec. 2, and the method adopted for its solution, which is a straightforward extension of the usual analysis of perturbation theory graphs, is described in Sec. 3. Two simple examples are treated in Sec. 4, while in Secs. 5 and 6 we study the less trivial cases of the triangle graph as a function of each of two external invariants. In Sec. 7 the technique is recapitulated and we comment on the results.

2. FORMULATION OF THE PROBLEM

We now have to formulate more precisely the aim outlined in the Introduction. Let us illustrate our approach in a simple way by considering the well-known example of approximating, by a resonance pole, the two-particle scattering amplitude itself $F(W^2)$, where W^2 is the c.m. system energy of the particles. Figure 1 represents the scattering of two particles A and B of unit mass (in what follows *all* particles are scalars and of unit mass, for convenience) via two-particle intermediate states which include all interactions of the particles; we call the internal part of Fig. 1(a), shown

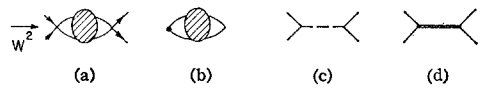

FIG. 1. (a) The two-particle scattering amplitude; (b) the two-particle Green's function, G; (c) Fig. 1(a) with G replaced by a line of mass λ; (d) the resonance approximation to Fig. 1(a), in which G in Fig. 1(a) is replaced by a line of complex mass.

* Work performed under the auspices of the U. S. Atomic Energy Commission.

† Present address: Service du Physique Theorique, C.E.N., Saclay, France.

‡ Present address: University of Maryland, College Park, Maryland.

[1] S. Mandelstam, J. E. Paton, R. F. Peierls, and A. Q. Sarker, Ann. Phys. (N. Y.) **18**, 198 (1962).

[2] D. Zwanziger, Phys. Rev. **131**, 888 (1963).

[3] R. C. Hwa, Phys. Rev. **130**, 2580 (1963).

[4] G. Bonnevay, Nuovo Cimento (to be published).

in Fig. 1(b), the two particle Green's function $G(W^2)$. The part of F which contains G is related to G by various constants, and kinematical factors for the external lines, with which we shall not be concerned; hence its structure is given by that of G, which is assumed to satisfy a Lehmann spectral representation. Hence, for Fig. 1(a) we have

$$F(W^2)=(1/\pi)\int_{\lambda_0^2}^{\infty} d\lambda^2 \frac{\sigma(\lambda^2)}{W^2-\lambda^2+i\epsilon}, \qquad (2.1)$$

where $\sigma(\lambda^2)$ is a spectral function associated with the intermediate states to which A and B are coupled, and the integral is along the real axis from the square of the mass λ_0^2 of the lowest two-particle intermediate state. At this stage, σ is real, non-negative, has a cut from λ_0^2 to ∞, and its behavior at ∞ is such that (2.1) converges; some further properties of σ will be given below.

In general, of course, A and B may be coupled to a stable single-particle state also; one would then add to (2.1) a pole term at a mass M^2 below λ_0^2. In some region of the physical range of W^2, it might be that this pole term, $1/(W^2-M^2)$, would dominate the scattering; this is the basis of "pology." [This term is included in the form (2.1) by taking the integral from 0 to ∞, over a spectral function which has a delta function singularity at $\lambda^2=M^2$ and which is σ beyond λ_0^2.] Suppose now that no such term is present, but that, rather, σ has a pair of complex conjugate poles, on all sheets, at $\lambda^2=I^2$ and $\lambda^2=I^{*2}$, where $\mathrm{Im}I^2$ is less than zero, and $\arg(I^2-\lambda_0^2)\approx 0$. That is, we assume that σ has the form

$$\sigma(\lambda^2)=(\lambda^2-\lambda_0^2)^{\frac{1}{2}}r(\lambda^2)/(\lambda^2-I^2)(\lambda^2-I^{*2}),$$

where r is a function regular in the right half-plane. The cut is only tied down to λ_0^2, and in our applications it will be deformed as necessary; it will not be mentioned further explicitly. In some simple theories,[5] it is known that this corresponds to the situation in which A and B have a resonance at $W=I$, whose width is related to $\mathrm{Im}I$. This resonance would then dominate the scattering in some region of W near $\mathrm{Re}I$. Recalling the form of the Breit-Wigner resonance formula, we might think that in a way analogous to the stable particle case, F may be approximated by a pole formula of the type $1/(W^2-I^2)$. In this case, however, as is well known, the pole is on the *second W^2 sheet*,[6] and thus F cannot be represented exactly by $1/(W^2-I^2)$. We shall see in Sec. 4 how this may be nevertheless a good approximation to F. Let us now, however, restate this result in a slightly more roundabout way which we shall then generalize. First, let us rewrite (2.1) as

$$F(W^2)=(1/\pi)\int_{\lambda_0^2}^{\infty} d\lambda^2\sigma(\lambda^2)f(W^2|\lambda^2),$$

[5] M. Levy, Nuovo Cimento **13**, 115 (1959).
[6] R. E. Peierls in *Proceedings of 1954 Glasgow Conference* (Pergamon Press, London, 1955), p. 296.

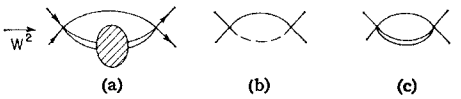

FIG. 2. (a) The two-particle scattering amplitude with three-particle intermediate states, only one pair interacting through the two-particle Green's function G.; (b) Fig. 2(a) with G replaced by a line of mass λ; (c) the resonance approximation to Fig. 2(a).

where $f(W^2|\lambda^2)=(W^2-\lambda^2+i\epsilon)^{-1}$. $f(W^2|\lambda^2)$ is just the Feynman graph for AB scattering, Fig. (1a), with G replaced by a single line of mass λ, as is shown in Fig. 1(c). The result may now be stated as follows: Replacing the internal G by the resonance mass I, as shown in Fig. 1(d), gives a singularity on the first sheet (in fact, on all sheets) of $f(W^2|I^2)$, but on the *second* sheet of $F(W^2)$.

We now generalize this. Let $f(x,y,\cdots|\lambda^2)$ be a Feynman graph in which all internal particles except one have unit mass, the remaining line having a mass λ; let $F(x,y,\cdots)$ be the function obtained by replacing this λ line, in $f(x,y,\cdots|\lambda^2)$, by the two-point function G. (The restriction to unit mass can, of course, be trivially relaxed; it is made for algebraic convenience only.) We shall often write simply F, and f or $f(|\lambda^2)$; $(x,y,\cdots)$ are the external variables of the problem. F corresponds to a sum of all graphs which have the form of f, but in which, in place of the λ line, all possible two-particle insertions are made. Then

$$F(x,y,\cdots)=(1/\pi)\int_{\lambda_0^2}^{\infty} d\lambda^2\sigma(\lambda^2)f(x,y,\cdots|\lambda^2). \qquad (2.2)$$

Our problem is: In what sense F is approximated by $f(|I^2)$, and, more generally, how are the properties of F related to those of $f(|I^2)$? We shall actually consider in detail only two examples. One is shown in Fig. 2(a), a three-particle part of $F(W^2)$ containing G within itself; in this case $f(W^2|\lambda^2)$ is the self-energy function of Fig. 2(b). The other example is Fig. 3(a): a triangle graph containing G internally. For this case, two variables enter, W^2 and s, and $f(s,W^2|\lambda^2)$ is the triangle graph of Fig. 3(b).

We have already seen one trivial example of how $f(W^2|I^2)$ may be singular on a given sheet while $F(W^2)$ is not. Very often, however, $f(x,y,\cdots|I^2)$ may be a useful representation of $F(x,y,\cdots)$ in a certain energy range. To illustrate our findings, and to whet the reader's appetite, we close this section by giving a rough outline of our results. In what follows we shall take all the elementary particles involved to be scalars and of equal unit mass.

Firstly, we point out that we shall clearly need the properties of $f(x,y,\cdots|\lambda^2)$ as, say a function of λ^2 as well as x. Hence we will have to analyze Feynman graphs with respect to an *internal* mass. $f(x,y,\cdots|\lambda^2)$ is a many-sheeted function, and so is $F(x,y,\cdots)$ as

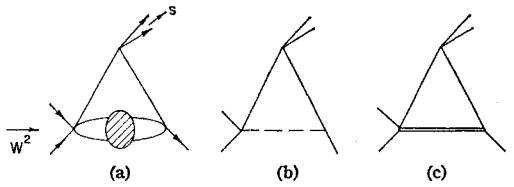

FIG. 3. (a) A rescattering, or triangle, graph containing G internally; (b) Fig. 3(a) with G replaced by a line of mass λ; (c) the resonance approximation to Fig. 3(a).

defined by (2.2). We postpone until the next section the detailed definition of the physical, first unphysical, etc. sheets, remarking here only that, roughly speaking, the physical sheet of $F(x,y,\cdots)$ is defined by integrating the physical sheet amplitude $f(x,y,\cdots|\lambda^2)$ along the undistorted λ^2 contour. Continuations to other sheets are then made by continuing $f(x,y,\cdots|\lambda^2)$ and by distorting the λ^2 contour. Two cases arise, depending on the choice of external variables used to analyze $F(x,y,\cdots)$, and a convention can be conveniently introduced from the examples of Figs. 1–3. For Fig. 3(b), the definition of the s physical sheet of $f(s,W^2|\lambda^2)$ is independent of λ^2, for all real $\lambda^2>\lambda_0^2$; it only depends on λ^2 through the end point λ_0^2 (see Sec. 3.1). We say that the resonance is in a "crossed" channel, since it appears in a channel crossed with respect to s. If we chose to analyze Fig. (3a) in terms of W^2, however, the W^2 physical sheet of Fig. 3(b) would depend on λ^2; the resonance is then said to be in a "direct" channel. Figures 1(a) and 2(a) are both, of course, direct channel cases.

For the crossed channel case we are able to give a complete treatment of the triangle graph, Fig. 3(a). We find, firstly, as already mentioned, that for certain W^2, $f(s,W^2|I^2)$, shown in Fig. 3(c), has a physical sheet singularity in s while $F(s,W^2)$ does not. Secondly, we find that for a certain range in $W^2\geq 9$, both $f(s,W^2|I^2)$ and $F(s,W^2)$ have a logarithmic singularity on the second sheet below the s cut rather close to the physical region,[7] leading to a peak in $F(s,W^2)$ near the s threshold. Finally, we show how to reach all the singularities of $F(s,W^2)$ for a general W^2, on all s sheets, due to the resonance poles I^2 and I^{*2}. (It is convenient to introduce the general shorthand name "resonance singularity" for all such singularities.) Resonance singularities associated with I^{*2} are never near the physical region.

In the direct channel case, we analyze the somewhat trivial Figs. 1(a) and 2(a) completely, obtaining the well-known results of, in the one case, a second sheet resonance pole in W^2, at $W^2=I^2$, and in the other, a second sheet resonance square-root branch point in W^2 at $W^2=(I+1)^2$. For Fig. 3(a) as a function of W^2, however, we are not able to give a complete discussion. The difficulty is primarily that the properties of $f(s,W^2|I^2)$ are defined with respect to a *complex* branch point $W^2=(I+1)^2$. We investigate the physical and nearest unphysical regions of $F(s,W^2)$, but do not search further sheets; nor can we give a direct way of calculating effects in the physical region, although an indirect procedure does give a peak due to a resonance logarithmic singularity, the existence of which we are able to prove.

[7] This result has been found by G. Bonnevay, Ref. 4.

3. GENERAL METHODS

We wish to study the analytic structure of $F(x,y,\cdots)$, given by Eq. (2.2), as a function of one of $(x,y,\cdots)$ when the remainder are held constant. We first indicate the definitions of the physical and various unphysical sheets of $F(x,y,\cdots)$, and then describe two general methods useful in the analysis.

3.1. The Physical and Unphysical Sheets of f and F

Let us write F and f for $F(x,y,\cdots)$ and $f(x,y,\cdots|\lambda^2)$, respectively. We recall that f is a standard perturbation theory graph containing an internal particle of mass λ; it is a many-sheeted function. Suppose we are interested in the properties of F in the x plane. Then we first of all have to define a physical x sheet, for f, by drawing cuts from branch points due to the lowest contraction of f, then the next lowest, and so on successively up to the (leading) singularity of f itself. It is evident from (2.2) that this physical sheet is to be defined in the complex space of x, say, *and* λ^2. We are at once faced with a problem involving two complex variables. Two cases arise. In the first, which we call the crossed-channel case for reasons which will emerge later, singularities in x and in λ^2 from the lowest nontrivial contractions of f—self-energy graphs—are independent of each other. Let these singularities be at x_i and λ_i^2, and draw cuts in the x and λ^2 planes from x_i and λ_i^2 so as to define independent Riemann sheets in the λ^2 and x planes. Then f is defined in the topological product of the two cut planes, and the sheets of f are with respect to these (independent) cuts in the x and λ^2 planes. Let us call the first sheet with respect to these cuts the physical sheet p, and denote by q the first unphysical sheet. In the x plane, p and q are defined with respect to a cut from the normal threshold x_0, going along the real axis to $+\infty$. The definition of the λ^2 sheets will be given in Sec. 4.1. Finally, let us denote by f_{pq}, etc., the function f when x is in its physical sheet p, and λ^2 is in its sheet q, etc.; as a convention, we always refer to the external variable x first in the subscript.

Now as far as F is concerned, in this crossed-channel case, it certainly has the singularity x_0 since that is independent of λ^2; we draw a cut from x_0 to ∞ along the real axis. The physical amplitude F is then obtained from (2.2) by integrating, with $x>x_0$ approaching the real axis from above, the physical amplitude f_{pp}, along a λ^2 contour just below the real axis [cf. the $+i\epsilon$ in (2.1)], from λ_0^2 to $+\infty$. The physical sheet P of F is then defined initially by continuation, in a counter-

clockwise sense with respect to x_0, from this region near the real axis into the complex plane without completely encircling $x=x_0$. The λ^2 contour has to be deformed if necessary. This continuation will certainly be unique if there are no other singularities of the physical sheet amplitude—for example, anomalous thresholds—located off the real axis. For the crossed-channel case which we consider—the graph of Fig. 3(a) as a function of s—this is true, although $f_{pp}(s,W^2|\lambda^2)$ does have a logarithmic singularity *on* the real s axis, on the lower edge of the s cut; this then leads, as we shall see, to a singularity of $F(s,W^2)$ on P just below the real axis at, say, $s=s_a$. Hence a complete definition of P must include a specification of the cut attached to s_a, and we shall take it to be simply along the real axis below the normal threshold cut.

It is actually now already evident that f_{pp} may be singular at some complex point, while F is nevertheless not singular on P. The condition is simply that in the continuation of x into P we never have to distort the λ^2 integration contour. We shall return to this below in Sec. 3.2.

We have now defined F throughout the physical sheet P for the crossed-channel case. A second case arises, however, if the singularities in x and λ^2 from the lowest order contraction are not independent of each other; that is, $\lambda_i=\lambda_i(x)$ and $x_i=x_i(\lambda^2)$. Then it is no longer true that f may be regarded as an analytic function in the simple topological product of two cut planes. While our approach does not break down completely, our treatment will be less complete. In this case, we have to analyze first of all how the singularity x_1 survives the λ^2 integration. The details of this we postpone till Sec. 3.2, but the result is that it is only $x_0=x_0(\lambda_0^2)$ which is a singularity of F. A cut along the real axis from x_0 then serves to define P initially, provided there are no complex singularities.

Suppose we now start from a point in the physical region ($x>x_0$ and above the real axis), and continue in a clockwise sense with respect to x_0 across the cut. The sheet reached on this path will be called Q and is the unphysical sheet nearest to the physical region. We shall now be integrating f_{qp}, and in performing this continuation singularities may appear in f and move towards the λ^2 contour, forcing us to distort it, a process which will be halted when a singularity of F, pushing the contour in front of it, meets a singularity of σ. Then we will find a singularity of F in Q, so that Q will have to be defined by an additional cut starting from this and any other singularities we find in a similar way. Further sheets $(R,S,\cdots)$ can then be defined by various other paths of continuation. As for f, we denote by $(F_P,F_Q,\cdots)$ the function F on sheets $(P,Q,\cdots)$.

We now go on to describe in more detail a method, the rough outlines of which we have just given, for finding the singularities of P on the various sheets. We call it the search method.

3.2. The Properties of F

3.2a. The Search Method

This is based on the now well-known method of Hadamard[8–10] for obtaining the domain of holomorphy of a function defined by some integral representation. We follow an arbitrary path in the many-sheeted complex x plane, and see how far we may enlarge the domain of holomorphy of F, by distorting, if necessary, the λ^2 contour away from an advancing singularity of f. This enlargement proceeds unless (i) a λ^2 singularity of f coincides with λ_0^2, or with $\lambda^2=\infty$; or (ii) a pair of λ^2 singularities of f are coincident and pinch the λ^2 contour; or (iii) a λ^2 singularity of f pinches the λ^2 contour against a singularity of σ. That one of the three alternatives (i) to (iii) is the case is necessary, though not, in general, sufficient, for the existence of a singularity of F.

The singularities of σ which are our immediate concern are $\lambda^2=I^2$, and $\lambda^2=I^{*2}$. The σ branch point at $\lambda^2=\lambda_0^2$ has already been considered in (i). The singularities arising by (i) and (ii) define the physical sheet of F, and those arising by (iii) are then to be determined with respect to this physical sheet. To determine the sheets on which the resonance singularities are found, we must follow the deformations of the λ^2 integration contour, in order to see that the coincident singularities actually pinch the λ^2 contour. To repeat, it is now clear that if throughout P no deformation of the λ^2 contour is necessary, F_P will have no complex singularities although $f_{pp}(x,y,\cdots|I^2)$ may be singular.

We shall normally use the search method, but there is another which we describe briefly.

3.2b. The Dispersion Method

This is based on dispersion theory. We express f as a dispersion integral in x with a spectral function $\phi(x|\lambda^2)$, that is

$$f(x,y,\cdots|\lambda^2)=(1/\pi)\int_{C(y\cdots|\lambda^2)}\frac{dx'}{x'-x-i\epsilon}\phi(x',y\cdots|\lambda^2), \quad (3.1)$$

where C represents the integration contour. Then

$$F(x,y\cdots)=(1/\pi)\int_{C(y\cdots)}\frac{dx'}{x'-x-i\epsilon}\Phi(x',y\cdots), \quad (3.2)$$

where

$$\Phi(x,y\cdots)=\int_{\lambda_0^2}^{\infty}d\lambda^2\sigma(\lambda^2)\phi(x,y\cdots|\lambda^2). \quad (3.3)$$

Singularities of Φ in x give rise to singularities of F on Q.

[8] R. J. Eden, Proc. Roy. Soc. (London) **A210**, 388 (1952) was the first to apply the method of J. Hadamard [Acta Math. **22**, 55 (1898)] to this type of problem.
[9] J. Tarski, J. Math. Phys. **1**, 149 (1960).
[10] L. F. Cook and J. Tarski, J. Math. Phys. **3**, 1 (1962).

We arbitrarily distort the λ^2 contour in (3.3), in such a way that we explicitly separate off the contribution of the pole of σ at $\lambda^2=I^2$,

$$\Phi(x,y\cdots)=\hat{\Phi}-2\pi iR\phi(x,y\cdots|I^2), \qquad (3.4)$$

where R is the residue of σ at the pole $\lambda^2=I^2$. By this separation it seems that Φ contains $\phi(x,y\cdots|I^2)$ and thus the singularities of $\phi(x,y\cdots|I^2)$. These singularities may give rise to singularities of F on Q. However, we must ensure that the singularities of ϕ are not cancelled by those of $\hat{\Phi}$.

This method has certain difficulties of execution, though not of principle, and in general we prefer the search method. To proceed with it we have to know the properties of $f(x,y,\cdots|\lambda^2)$ as a function of λ^2.

3.3. Properties of f

Before dealing with F we must know the singularities of $f(x,y,\cdots|\lambda^2)$ in λ^2 for all complex λ^2 and x, say, the other variables $(y,\cdots)$ being real and physical. This requires the study of the analytic properties of perturbation theory graphs as a function of two complex variables, one being an internal mass and the other an external variable. This has only once before been studied, in a rather different context.[11] We apply here two methods more usually used for the analysis of two external variables, namely perturbation theory and dispersion methods.

The perturbation theory analysis is a fairly obvious generalization of the methods developed by Eden,[8] Tarski,[9] and Cook and Tarski,[10] though several unusual features arise. We write the standard integral over Feynman parameters α_i, and find the various (x,λ^2) surfaces on which end point or coincident singularities of the α_i integrations occur. The singularity character of such a surface can only change at contact with the "one further contraction" surface, and theorems (3.2) and (3.3) of Ref. 10 can easily be generalized for variables (x,λ^2). A slightly unusual feature is that the lowest order singularity surfaces are given by $\alpha_k=1$, $\alpha_i=0$, all $i\neq k$. One must also take account of the possible second type singularities.[12] The treatment of a leading singularity curve in (x,λ^2) is straightforward provided the physical sheet defined by the lower order singularities does not contain any complex singular surfaces which depend on both x and λ^2. This is the basis of the distinction between crossed and direct variables, and we do not pursue the treatment of direct variables as vigorously as that of the (simpler) crossed variables.

The analysis of $f(x|\lambda^2)$ can also be performed by dispersion methods, if f satisfies a dispersion relation in x with a spectral function ϕ whose properties are known as a function of x for at least some range of λ^2. One can then obtain the properties of $f(x|\lambda^2)$ by continuing ϕ in λ^2. Whenever a singularity in x of ϕ crosses the x dispersion integration contour, this leads to a new singularity of f. Continuation in x onto other sheets is done by deforming the x integration path as necessary, so that x singularities of ϕ become second-sheet singularities of f. For the triangle there is no lack of dispersion relations[13]; however this method of analysis requires care in keeping account of sheets. The same problems of lower order singularities arise here as for the perturbation theory method, when these lower singularities depend on both variables. Thus we prefer the method of perturbation theory. (The two methods should always lead to the same results.)

For actual calculations, however, once the singularities have been determined, we shall use dispersion theory; we now give an outline of this.

3.4. Calculation of F

The case in which a resonance singularity is most interesting is when F_Q has a singularity just below the real axis, since then it is near the physical region in P; it is for this case that we shall calculate F. The method can certainly be generalized.

Suppose F_Q has a resonance singularity at x_I, say, due to a pinch between the pole of σ and a singularity of $f_{\alpha\beta}$, where α, β stand for the x, λ^2 sheets of f. Then

$$F_Q=\hat{F}_Q-2iR(I^2)f_\alpha(x,y,\cdots|I^2), \qquad (3.5)$$

where $R(I^2)$ is, as before, the residue of the pole in σ at $\lambda^2=I^2$, and where $\hat{F}$ has a definition similar to that of F_Q except that the λ^2 contour passes below $\lambda^2=I^2$. The λ^2 index on f has been dropped for clarity since it will be p in our calculations. Then $\hat{F}_Q$ has no singularity at x_I, since the λ^2 contour is not pinched; the singularity of F_Q at x_I is in $f_\alpha(x,y,\cdots|I^2)$. In Q, we draw a cut from x_I to $+\infty$; let us denote by square brackets discontinuities across this cut. We then have the immediate result that, apart from constant factors,

$$[F_Q]=[f_\alpha(|I^2)]. \qquad (3.6)$$

To evaluate $[f_\alpha(|I^2)]$ we can use either perturbation or dispersion methods and we will use the latter. [We notice how this section is closely related to Sec. 3.2(b).]

In summary, we see that once we have proved that F has a singularity on Q at x_I, the effect of this can be calculated from the separated-off resonance contribution $f_\alpha(|I^2)$. The nontrivial part is to show that this contribution is not cancelled by the remaining "background" term $\hat{F}$.

4. TWO SIMPLE EXAMPLES

In order to clarify our methods, we now turn to some straightforward examples.

[11] J. Bronzan and C. Kacser, Phys. Rev. **132**, 2703 (1963).

[12] D. B. Fairlie, P. V. Landshoff, J. Nuttall, and J. C. Polkinghorne, J. Math. Phys. **3**, 594 (1962); Phys. Letters **3**, 55 (1962); also see, M. Fowler, J. Math. Phys. **3**, 936 (1962); Nuovo Cimento **27**, 952 (1963).

[13] C. Fronsdal and R. E. Norton, UCLA preprint, 1963 (unpublished).

4.1. The Two-Particle Amplitude with Two-Particle Intermediate States

As we have seen, the two-particle amplitude of Eq. (2.1)—Fig. 1(a)—can be identified with the form (2.2) by setting

$$f(W^2|\lambda^2)=1/(W^2-\lambda^2+i\epsilon). \tag{4.1}$$

$f(W^2|\lambda^2)$ is shown in Fig. 1(b). For σ we take only two-particle contributions, assuming, in particular, the existence of resonance poles I^2 snd I^{*2} as discussed in Sec. 2. As a function of the two complex variables W^2 and λ^2, f has a pole in each variable located at the value of the other variable (the $i\epsilon$ can be ignored). In this simple case f is not many sheeted. The physical sheet P of F is defined originally as the sheet for which the λ^2 integration runs on the real axis from 4 to ∞; thus on this sheet $F(W^2)$ has a continuum of poles, that is a cut, from $W^2=4$ to ∞, and the physical limit is obtained by approaching the real axis in the sense $W^2+i\epsilon$, i.e., from above. As we continue onto the second sheet Q of F through this cut from above, the λ^2 pole of f at $\lambda^2=W^2$ will cross the λ^2 integration path from above, unless we deform the contour downwards to avoid it. As W^2 approaches I^2, the deformed λ^2 contour is pinched between the pole of f at $\lambda^2=W^2$, and the pole of σ at $\lambda^2=I^2$, so that $W^2=I^2$ is a singularity of $F(W^2)$ on its second sheet [note that $W^2=I^2$ is a singularity for "all sheets" of $f(W^2|I^2)$]. This singularity is actually a pole, as can be seen if we follow the deformation of the λ^2 contour by two distinct W^2 paths to the same W_0^2, which pass $W^2=I^2$ clockwise and anticlockwise. One easily sees that the value of the λ^2 integration is the same for both paths. Of course an easier way is to write the λ^2 deformed contour as the original contour together with a closed loop about $\lambda^2=W^2$, as in Sec. 3.4, Eq. (3.5); we obtain

$$F_Q(W^2)=F_P(W^2)-2iR(I^2)f(W^2|I^2),$$

where we recall that F_P and F_Q are the values of F on its first (physical) and second sheets, P and Q, respectively. One can go on to find the $W^2=I^{*2}$ second-sheet singularity (a pole); and also to show that going through the second-sheet cut from above returns us to the first sheet, so that $W^2=4$ is a square-root branch point, which is a consequence of the two-sheeted nature of $\sigma(\lambda^2)$.

$F(W^2)$ is a two-sheeted function, while $f(W^2|\lambda^2)$ is single valued. $f(W^2|I^2)$ has a pole which corresponds to that second-sheet pole of $F(W^2)$ which is *near* the physical edge of the physical sheet of F. Further, the behavior of $F(W^2)$ along this edge is properly reproduced by that of $f(W^2|I^2)$, both in magnitude and phase (disregarding a smooth background variation). On the other hand, $f(W^2|I^{*2})$ does *not* reproduce the physical value of $F(W^2)$ correctly (it gives the opposite phase); this is because the pole of $f(W^2|I^{*2})$ leads to a second-sheet pole of $F(W^2)$ which is *far* from the physical region, so that the physical values of $F(W^2)$ are incorrectly represented by $f(W^2|I^{*2})$, even to modulo a background term.

This trivial example, therefore, already demonstrates the necessity for caution in applying the resonance approximation, and shows that the important question is the location of the singularities of $F(W^2)$, not primarily those of $f(W^2|I^2)$ and $f(W^2|I^{*2})$.

4.2. The Two-Particle Amplitude with Three-Particle Intermediate States

To discuss resonance approximations to the three-particle intermediate state part of the two-particle amplitude, we analyze Figs. 2(a) and 2(b). In this case $f(W^2|\lambda^2)$ is the single-loop self-energy function, whose properties are well known for fixed real values of the internal masses (λ and 1 in our case). In particular, the explicit form of f is easily evaluated; the extension to complex λ^2 can be done either from the explicit form or by means of the dispersion relation satisfied by $f(W^2|\lambda^2)$.

Nonetheless, in order to demonstrate our general methods, we have treated f in full detail by the methods of perturbation theory. This analysis, which is given in Appendix A, will have a later application, since the self-energy function is a lower order (contraction) singularity of the triangle graph.

4.2a. Properties of Fig. 2(a) by the Search Method

We now turn to the properties of Fig. 2(a), given by

$$F(W^2)=(1/\pi)\int_4^\infty d\lambda^2\sigma(\lambda^2)f_{pp}(W^2|\lambda^2), \tag{4.2}$$

where $f_{pp}(W^2|\lambda^2)$ is Fig. 2(b); the indices will often be suppressed.

The properties of f that we use are proved in the Appendix. For a given real $\lambda^2>4$, $f(W^2|\lambda^2)$ has a W^2 cut running along the real axis between the two inverse square-root branch points at $W^2=(\lambda+1)^2$ (this is a direct channel case) and $W^2=\infty$, and the physical limit is from above this cut ($W^2=0$ is not a physical sheet singularity). $F(W^2)$ is defined in (4.2) with a real λ^2 path of integration. F has, firstly, a logarithmic singularity at $W^2=9$, where the singularity of f at $W^2=(\lambda+1)^2$ coincides with the end point $\lambda^2=4$. The physical sheet P of F is defined by a cut along the real W^2 axis running from 9 to infinity. This is the normal branch cut corresponding to the three-particle intermediate state. Commencing with any W^2 infinitesimally above this cut, W^2 can range throughout the whole complex plane avoiding the cut—that is, staying on P—and no singularity of $f(W^2|\lambda^2)$ will ever meet the λ^2 integration contour, since the singularities are at $\lambda^2=0$, $\lambda^2=-\infty$, and $\lambda^2=(W-1)^2$. Hence (a usual feature) the entire physical sheet definition of F is in terms of an undistorted λ^2 contour.

We now continue from the physical region of the W^2 physical sheet P onto the first unphysical sheet Q, and ask for the singularities of F_Q. For this continuation, we still integrate f, but the contour may have to be deformed since f now develops complex singularities [see the remarks following Eq. (A4)]. Exactly as in (4.1), we find that $W^2=(I+1)^2$ is a singularity of F_Q, due to a pinch of the λ^2 contour between the λ^2 singularity of $f(W^2|\lambda^2)$ at $\lambda^2=(W-1)^2$ and the pole of σ at $\lambda^2=I^2$. It is, in fact, a square-root branch point.[2] As W^2 continues clockwise on Q other possible singularity candidates are for $W^2=1$, at which the previously singular $\lambda^2=(W+1)^2$ passes through the $\lambda^2=0$ cut, and the second type singularity at $W^2=0$. Both of these are reasonably far from the physical region, and we do not pursue them further. If W^2 continues around on Q between $W^2=1$ and $W^2=9$, one finally encounters the singularity $W^2=(I^*+1)^2$. A singularity at $(I^*+1)^2$ can also be found on a search which starts on P below the real axis with $W^2>9$, and moves anticlockwise with respect to $W^2=9$, crossing the cut. Now, however, since $W^2=9$ is a logarithmic, not a square-root branch point, we reach a third sheet R, not Q, and the value of F_R is not that of F_Q. Again, one can reach $(I+1)^2$ on R. Other sheets can be defined similarly, but the singularities on them, and of F_Q at $(I^*+1)^2$, are far from the physical region, and we shall be mainly concerned with the singularity of F_Q at $(I+1)^2$. We remark that all these resonance singularities correspond to *first* sheet singularities of $f(W^2|I^2)$ and $f(W^2|I^{*2})$.

We now investigate the resonance singularities in Q more closely, show that they are branch points, and calculate the discontinuity associated with each. We let W^2 search to some W^2 on sheet Q, to the right of $W^2=(I+1)^2$, along two paths which pass $W^2=(I+1)^2$ in a clockwise and in an anticlockwise sense, obtaining $F_Q(W^2+)$ and $F_Q(W^2-)$. The appropriate λ^2 contours are shown in Figs. 4(a) and 4(b). One readily finds

$$\begin{aligned} F_Q(W^2+)-F_Q(W^2-) &= -2\pi i R(I^2)[f(W^2|I^2-)-f(W^2|I^2+)] \\ &= -2\pi i R(I^2)[f(W^2+|I^2)-f(W^2-|I^2)], \end{aligned} \tag{4.3}$$

where $R(I^2)$ is the residue of $\sigma(\lambda^2)$ at $\lambda^2=I^2$, and $f(W^2\pm|I^2)$ are the values of $f(W^2|I^2)$ obtained for W^2 passing clockwise and anticlockwise around the branch point of $f(W^2|I^2)$ at $W^2=(I+1)^2$. The form of (4.3) is again a special case of Eq. (2.7).

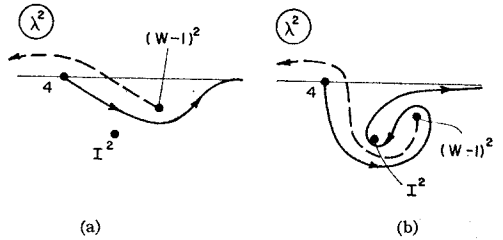

FIG. 4. The λ^2 contour and cut (dashed) for $F(W^2)$. (a) W^2 circling clockwise about $(I+1)^2$; (b) W^2 circling $(I+1)^2$ anticlockwise.

We can obtain the discontinuity of $f(W^2|I^2)$ by continuation in λ^2 from real to complex values; or directly using perturbation theory methods[14,15] (for we know that the discontinuity of f is due to one of the α_1 poles crossing the α_1 integration path); or by dispersion theoretic methods. We adopt the last (they all give the same result) since we can at the same time demonstrate the dispersive method of studying F.

4.2b. *Properties of $F(W^2)$ by the Dispersive Method, and Calculation of the Resonance Peak*

We have, as before,

$$F(W^2)=(1/\pi)\int_4^\infty d\lambda^2\sigma(\lambda^2)f(W^2|\lambda^2), \tag{4.4}$$

but now use the dispersion relation valid for real $\lambda^2>0$

$$f(W^2|\lambda^2)=\frac{1}{\pi}\int_{(\lambda+1)^2}^\infty \frac{dW'^2}{W'^2-W^2-i\epsilon}\phi(W'^2|\lambda^2), \tag{4.5}$$

with

$$\phi(W^2|\lambda^2)=[W^2-(\lambda-1)^2]^{1/2}[W^2-(\lambda+1)^2]^{1/2}/2W^2. \tag{4.6}$$

Then

$$F(W^2)=\frac{1}{\pi}\int_9^\infty \frac{dW'^2}{W'^2-W^2-i\epsilon}\Phi(W'^2), \tag{4.7}$$

with

$$\Phi(W^2)=\int_4^{(W-1)^2} d\lambda^2\sigma(\lambda^2)\phi(W^2|\lambda^2). \tag{4.8}$$

Singularities of Φ for complex W^2 give singularities of F on its second sheet. Equation (4.8) originally applied for $W^2>9$, with the λ^2 contour along the real axis. We continue in W^2, and obtain a singularity of Φ if (i) the end point $\lambda^2=(W-1)^2$ encounters a λ^2 singularity of ϕ or of σ, or (ii) two singularities of ϕ, or of σ, or one of σ and one of ϕ pinch the λ^2 contour (which may have been pushed by one of these). Notice that possible singularities arising from coincidences (ii) require a careful tracking of the deformations of the λ^2 contour to test for pinching. Hence, in general problems this method is less straightforward than the search method for finding singularities, though as we shall see below, it is very powerful for calculating observable effects. For the self-energy graph, the enumeration of possible singularities is straightforward. One finds (considering only I^2) that the end point meeting the pole of σ gives $(W-1)^2=I^2$ as a singularity, and the coincidence of ϕ and σ singularities gives the possibility of $W^2=(I-1)^2$. The latter is actually a singularity if W^2 first circles $W^2=(I+1)^2$,

[14] R. J. Eden, in *Brandeis Lectures in Theoretical Physics, 1961 Lectures* (W. A. Benjamin, Inc., New York, 1962), Vol. 1.
[15] R. E. Cutkosky, J. Math. Phys. 1, 429 (1960).

but not on a direct path. $W^2=0$ is also a singularity of both ϕ and of Φ, being the second type singularity.

We now distort the W'^2 path in (3.12), avoiding the singularities of Φ as shown in Fig. 5. The spectral function along C_1 is the straightforward continuation of Φ to complex W^2 for $(W-1)^2$ passing below $\lambda^2=I^2$; and the λ^2 integration along C_2 is equivalent to a λ^2 integration from $(I+1)^2$ to ∞, with a weight function

$$\Phi(W^2+)-\Phi(W^2-)=-2\pi i R(I^2)\phi(W^2|I^2). \quad (4.9)$$

But

$$\frac{1}{\pi}\int_{(I+1)^2}^{\infty}\frac{dW'^2}{W'^2-W^2-i\epsilon}\phi(W'^2|I^2)=f(W_+^2|I^2). \quad (4.10)$$

Therefore, for W^2 in the lower half-plane,

$$F_Q(W^2)=(1/\pi)\int_{C_1}\{dW'^2\Phi(W'^2)/(W'^2-W^2-i\epsilon)\} -2\pi i R(I^2)f(W_+^2|I^2), \quad (4.11)$$

where F_Q is the second-sheet continuation of F, the resonance contribution being explicitly separated off [it is clear that the C_1 integration has no singularity at $W^2=(I+1)^2$]. This is another example of the separation of the resonance contribution, as described in Sec. 3.4. If we now evaluate (4.11) for $W^2>9$, W^2 having an infinitesimal negative imaginary part, then the C_1 contribution will have a threshold behavior coming from $W^2=9$, but no other "peaking;" however, $f(W^2|I^2)$ will show some enhancement arising from the singularity at $W^2=(I+1)^2$. But $F_Q(W^2-i\epsilon)=F_P(W^2+i\epsilon)$; hence we see that the *physical* amplitude in the physical limit will show an enhancement due to the second-sheet singularity at $W^2=(I+1)^2$, which can be *calculated* simply from the resonance contribution of (4.11), which itself can be calculated from (4.5) and (4.6). Of course we cannot calculate the magnitude of the smoothly varying background term arising from the C_1 integration, but we do know that it does not cancel the resonance singularity. This enhancement is a woolly cusp effect of the type discussed by Nauenberg and Pais.[16]

5. THE TRIANGLE GRAPH WITH A RESONANCE IN THE CROSSED CHANNEL

Having outlined the general approach, and having used it in two simple examples, we now apply it to a rather less trivial case: the analysis of the triangle graph $F(s,W^2)$, Fig. 3(a), as a function of s. This is our first crossed channel case. As before, we write

$$F(s,W^2)=\int_4^{\infty}d\lambda^2\sigma(\lambda^2)f(s,W^2|\lambda^2), \quad (5.1)$$

where f is Fig. 3(b). We wish to find the connection between F and $f(|I^2)$, Fig. 3(c). We begin with the definitions of the physical, and first unphysical, sheets of F; that is, P and Q, respectively.

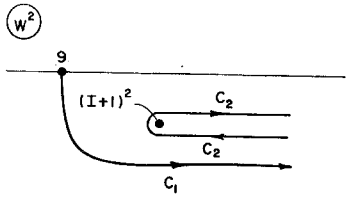

FIG. 5. The distorted W^2 dispersion integral path for $F(W^2)$. The part C_1 gives $\hat{F}$, with no singularity close to the physical sheet, while C_2 leads to an explicit separation of $f(W^2|I^2)$.

5.1. The Definition of Sheets P and Q

We first have to define the sheets of f, which in this case is rather more complicated, since f is a function of two complex variables, s and λ^2. For a given W^2, we need the complete analytic structure of f in λ^2 as well as s. This is derived in Appendix B. For the purposes of the present discussion, we first recall the notation for the sheets of f introduced in Sec. 3. The physical sheet of f is defined initially with respect to the various singularities coming from the contracted graphs, which in this case are self-energy graphs of the type of Fig. 2(b); these have been analyzed already in Appendix A. In the s plane, the physical sheet p is defined with respect to the normal threshold cut starting at $s=4$; the first unphysical sheet q is reached by crossing this cut from above. In the λ^2 plane, two cuts define the physical sheet p; they are drawn along the real axis from $\lambda^2=(W-1)^2$ to $-\infty$, and from $\lambda^2=0$ to $-\infty$ (these overlap, of course). If we cross the cut between $\lambda^2=0$ and $\lambda^2=(W-1)^2$ we pass to sheet q in λ^2, the $\lambda^2=(W-1)^2$ branch point being a square root singularity. The singularity at $\lambda^2=0$ is logarithmic, and in general we will not continue through the negative real λ^2 axis. Then f_{pq}, for example, denotes f when s and λ^2 are on sheet p and q, respectively. These lowest order singularities in s and λ^2 are independent of each other, so that this is a crossed channel case: λ^2 is in a crossed channel with respect to s. Hence f is defined in the product of the cut s and λ^2 planes.

We can now define the sheets of F. Since F certainly has those singularities of f which are independent of λ^2, we see that F has a square root (normal threshold) branch point at $s=4$. The resulting two Riemann sheets join across a cut in the s plane, which we take to be along the real axis from $s=4$ to $s=+\infty$. The physical amplitude F is obtained from Eq. (5.1) by integrating, with s approaching the real axis from above, the physical sheet amplitude f_{pp} along a contour taken just *below* the real λ^2 axis [cf. Eq. (2.1)]. In this case, we note that the definition of the λ^2 contour gives the necessary prescription for passing the branch point of f_{pp} at $\lambda^2=(W-1)^2$, which, for all s and $W^2>9$, lies on the

[16] M. Nauenberg and A. Pais, Phys. Rev. 126, 360 (1962).

real λ^2 axis to the right of $\lambda^2=4$. The physical sheet P is reached by continuation from the physical region above the real s axis into the complex s plane, in a counter-clockwise sense with respect to $s=4$.

An important remark follows from the properties of f_{pp} derived in Appendix B. Since f_{pp} is totally free of singularities for $\mathrm{Im}s>0$, $\mathrm{Im}\lambda^2<0$, it follows that as s moves in the upper half-plane, there is no λ^2 singularity which can approach the λ^2 integration contour; i.e., for $\mathrm{Im}s>0$, the λ^2 contour is *not* distorted. This remains true for $s\in w_-$, and $s\in v_-$ [cf. Eq. (B5a)]. Finally as s enters u_- from v_- by crossing H_-, λ_-^2 does become singular; however, it enters p through L. $0\leq\lambda^2\leq 4$, thus avoiding the λ^2 contour. We therefore see that this continuation may proceed throughout the whole s plane without our having to distort the λ^2 contour, so that we may write, with an *undistorted* contour,

$$F_P=\int_4^\infty d\lambda^2\sigma(\lambda^2)f_{pp}(|\lambda^2). \tag{5.2}$$

To anticipate somewhat, we point out that this is not true for continuation into Q, the sheet reached by a clockwise continuation with respect to $s=4$; then we must write

$$F_Q=\oint_4^\infty d\lambda^2\sigma(\lambda^2)f_{qp}(|\lambda^2), \tag{5.3}$$

the circle sign on the integral indicating that a distortion of the λ^2 integral has been necessary.

Sheets P and Q will also have to be further defined with respect to additional branch points of F arising from pinch or end point singularities of the λ^2 integration. The initial definitions of P and Q are shown in Fig. 6.

5.2. Properties of F and Sheets P and Q

In addition to the λ^2-independent singularity at $s=4$, F_P or F_Q are singular, firstly, when one of the triangle singularities of $f_{pp}(s,W^2|\lambda^2)$, denoted by λ_+^2, λ_-^2, reaches the end points $\lambda^2=4$, $\lambda^2=\infty$, of the λ^2 integration. The motion and singular character of λ_+^2, λ_-^2 are described in Appendix B. We refer to Fig. 19 in particular, which defines certain regions, in the s and λ^2 planes, which we shall use frequently. From Eq. (B5) and Fig. 18 we see that as s approaches $\frac{1}{2}(W^2-1)$ through values greater than this, below the real axis (that is, as s tends to the upper left corner of u_-) a singularity λ_-^2 of $f_{pp}(W^2,s|\lambda^2)$ reaches the end point $\lambda^2=4$. Hence $s=\frac{1}{2}(W^2-1)$ is a singularity for F_P, reached from below the real axis (and is far from the physical region). In the same way, we find that $s=\frac{1}{2}(W^2-1)$ is a singularity

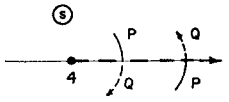

FIG. 6. The initial definition of the s physical (P) and nearest unphysical (Q) sheet, for F in the crossed channel case.

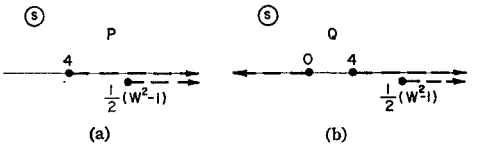

FIG. 7. (a) The physical (P) sheet cuts of $F(s,W^2)$; (b) some of the cuts of $F(s,W^2)$ on the nearest unphysical sheet Q.

for F_Q, reached from above the real axis. The fact that for $\lambda^2=4$ the singularities of f_{pp} coincide is essentially irrelevant. The existence of these singularities at $s=\frac{1}{2}(W^2-1)$ may also be inferred from a conventional analysis of $f_{pp}(W^2,s|4)$ in terms of W^2 and s (although this case is admittedly somewhat degenerate), or by explicitly making continuations of $F_P(F_Q)$ along two paths passing on either side of $\frac{1}{2}(W^2-1)$, starting from below (above) the real axis and ending above (below) it. These continuations lead to different results, demonstrating the existence of a singularity of F_P and F_Q at $\frac{1}{2}(W^2-1)$.

Finally, we remark that $s=0$ is not a singularity of F_P. At first sight we might suspect that it was, since if we make a circle about it inside w in the s plane, one of the λ^2 points, λ_-^2, crosses the λ^2 cuts near $\lambda^2=-\infty$, and hence its singularity character might change. This does not occur on this sheet, since this "possible" singularity cannot cause a deformation of the λ^2 contour in Eq. (5.1). Since $f_{pp}(s,W^2|\lambda^2)$ is certainly regular at $s=0$ for all λ^2 on the undistorted λ^2 contour, it follows that $s=0$ cannot be a singularity of F_p. [Of course, $s=0$ also arises by contraction of the λ^2 side of the triangle, as both the Landau pseudothreshold $(m_1-m_2)^2$, and also as the second type singularity. But these are not singular on the *physical* s sheet.]

In fact, one finds that $s=0$ and $s=-\infty$, the two singularities associated with $\lambda^2=\infty$, appear only in F_Q. Since any remaining singularities of F_P or F_Q come from a pinch of the λ^2 contour at $\lambda^2=I^2$ or I^{*2}, where I is complex, we have found all the branch points of F_P and F_Q on the real axis. Our choice of cuts for F_P and F_Q at this stage is shown in Fig. 7. Crossing a cut on two successive revolutions about $s=4$ returns us to the same sheet as that on which we started only if we cross in the region $4\leq s\leq\frac{1}{2}(W^2-1)$.

Consider now, for F_P, the possibility of a pinch at $\lambda^2=I^2$ or I^{*2}. On its physical sheet, f_{pp} may have complex singularities for s in u_-, if I^2 is in w_- [Eq. (5)]. But, as we remarked earlier, no deformation of the λ^2 contour in Eq. (5.1) is necessary to reach these points, nor is it necessary throughout P, so that no pinch can occur. That is, F_P has no complex resonance singularities, despite the fact that $f_{pp}(W^2,s|I^2)$ may have. The difference between the properties of F and those of $f(|I^2)$ is made clearly evident.

The situation is different for F_Q, however. Let us introduce the notation $Q(u_-)$ to denote the domain u_- on sheet Q, etc. . . . We shall illustrate the procedure

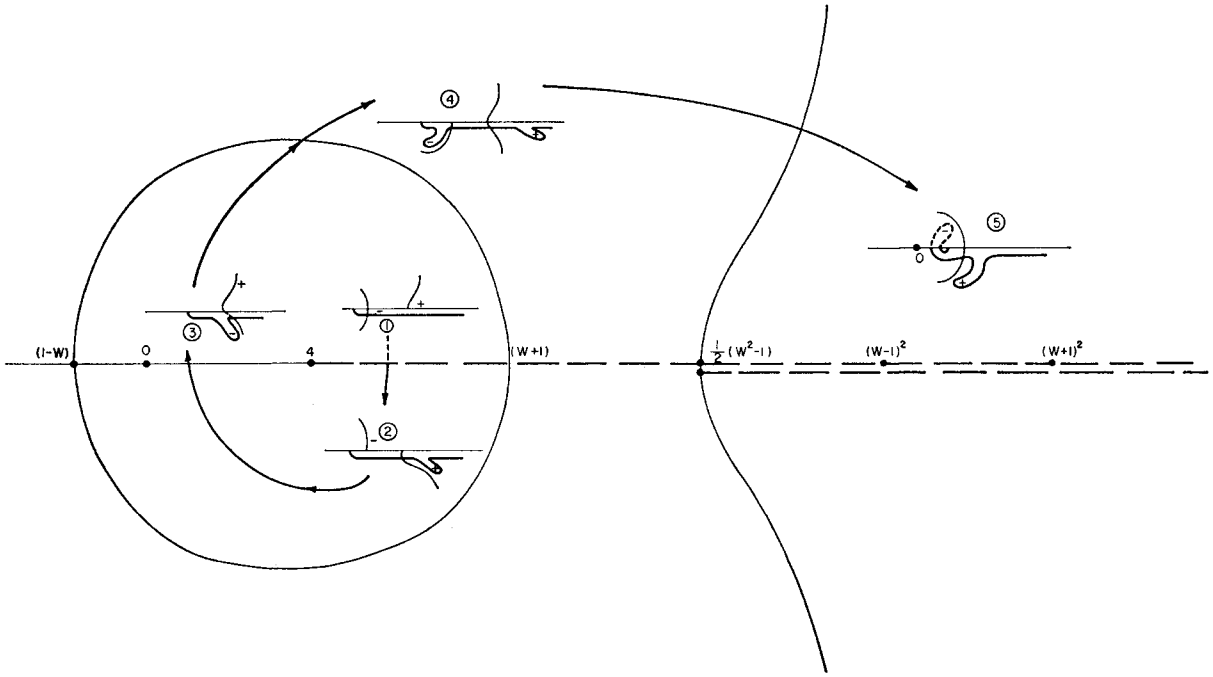

FIG. 8. A search for resonance singularities in the s variable of the triangle graph $F(s,W^2)$ (the crossed channel case). The search path in the s plane is shown by the heavy line joining ringed points on the path. The inset diagrams show the λ^2 plane at each ringed point. In these, the singularities in λ^2 of the triangle graph $F(s,W^2|\lambda^2)$ are shown by the plus and minus signs; the λ^2 contour is the heavy line. Only the essential parts of the bounding curves $S_\pm$, $H_\pm$ have been included. The cuts in the s plane are indicated by thick dashed lines. A detailed commentary on this figure is given in the text.

by one rather straightforward search, which we describe in detail. It is drawn in Fig. 8, and we shall devote the rest of this section to explaining, and commenting on, this diagram.

The over-all plane is the s plane for F, divided into the six regions $u_\pm$, $v_\pm$, $w_\pm$ as defined in Appendix B. This plane has two cuts along the real axis from 4 to ∞, and from $\frac{1}{2}(W^2-1)$ to ∞. [It also has two "naming" cuts (see Appendix B) between 0 and 4, and between $(W-1)^2$ and $(W+1)^2$.] Starting at the point 1 in $P(w_+)$, we cross the first cut, passing into $Q(w_-)$, and proceed to search for singularities along the route 2, 3, 4, 5. This route crosses no other cuts (at a naming cut, the name of the singularities of f, not their singular character, changes). Consideration of the sheets reached by crossing the cut attached to $\frac{1}{2}(W^2-1)$ will be deferred to Sec. 5.3. This route in the s plane is shown by the line joining the points 1–5; the part of that line in $P(w_+)$ is shown dotted, to emphasize that between points 1 and 2 we move from P to Q, so that it is on a different sheet of F from the remainder.

The insert diagrams, on the other hand, show the λ^2 plane. The regions $u_\pm$, etc., are indicated, as needed, by light solid lines. The positions of the two singularities of f, λ_+^2 and λ_-^2, are indicated by + and − signs; their singular character, and motion, is determined in Appendix B. In this plane, there are, we repeat, cuts along the real λ^2 axis from $(W-1)^2$ to $-\infty$, and from 0 to $-\infty$, which for clarity are not shown in the Fig. 8. Finally, the λ^2 contour, which runs initially from 4 to $+\infty$, just below the real axis, is shown as a heavy solid line.

We start at the point 1, in $P(w_+)$, so that Eq. (5.1) holds. Neither λ_+^2 nor λ_-^2 is singular for f_{pp}, and the λ^2 contour is undistorted. As we pass to 2, we move continuously onto Q, and onto the q sheet in s. We see that λ_+^2 has crossed a λ^2 cut, so that it now appears on f_{qp} [see Eq. (B6)], forcing a deformation of the contour down into u_-. *This is the crucial point of the whole analysis.* At 3, we cross a naming cut, and the names λ_+^2, λ_-^2 interchange; the properties of F_Q, however, remain the same. At 4, the distorted λ^2 contour now enters w_-, having passed through v_-, while at 5 it enters w_+. At 5, the distortion has forced a part of the contour through the λ^2 cut between 4 and 0, so that for that part we would be integrating f_{qq}. (cf. the remark at the end of Appendix B.) That part is shown dotted.

The possibilities for resonance singularities are now quite evident; we require the deformed λ^2 contour to collide with a pole of σ. We shall state the results. Most notably, we see that there is a complex singularity in $Q(w_-)$ if I^2 is in u_-.[7] This is near the physical region in $P(w_+)$ if the imaginary part of I is sufficiently small. We shall show how to calculate the effect of this singularity in Sec. 5.4, below. It is found on any path entering Q from P in the upper half-plane. Note that $s=W+1$ is not a branch point of F_P. It may appear, at first sight, that it is, since if we penetrate $Q(v_-)$ by going from

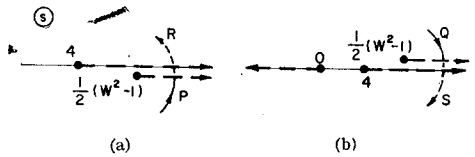

FIG. 9. (a) and (b). The location of the sheets R and S of $F(s,W^2)$.

$P(w_+)$ via $P(v_+)$, for instance, no λ_+^2 singularity appears in f_{qp} to force a λ^2 contour deformation, so that there is no singularity in $Q(v_-)$. However, if we then move into $Q(w_-)$, the singularity does appear; essentially, this is because as we circle $s=W+1$ *once*, the λ_+^2 point circles the $\lambda^2=(W-1)^2$ cut *twice*. $s=\frac{1}{2}(W^2-1)$ is not a branch point either, when approached from above the real axis, since, although the singular character of λ_-^2 does change, it causes no deformation of the contour. These comments reflect our earlier findings about the singularities of F on P, and the content of these is that, in general, any point in Q can be reached from P on an *arbitrary* path crossing the cut. Hence any most convenient search into Q is adequate for any given region.

The remaining results for sheet Q will be summarized below, in Sec. 5.3, where we investigate higher sheets of F.

5.3. Further Sheets of F, and Some Singularities on Them

Although $s=\frac{1}{2}(W^2-1)$ is not a singularity of F_P when reached from above the real axis, it is when reached from below, as we saw in Sec. 5.2. It is also a singularity of F_Q from above. Referring to Fig. 9, denote by R the sheet reached by continuing across the real axis into u_+ from $P(u_-)$; and by S that reached by continuing in the opposite sense into u_- from $Q(u_+)$. Both of these sheets are rather far from the physical region of P. Nevertheless there is some point in investigating them. Firstly, the analysis is easily handled by the search method, and is an example of a distinctly nontrivial case. Secondly, singularities associated with I^{*2} are frequent on these sheets. Thirdly, we recall that for the two-particle amplitude with three-particle intermediate states (Sec. 4.2), the resonance singularities were found by penetrating the cut attached to the branch point associated with $\lambda^2=4$; we might expect, therefore, as has been conjectured by Challifour,[17] that continuations through the cut attached to the branch point $s=\frac{1}{2}(W^2-1)$, associated with $\lambda^2=4$, would also find resonance singularities. We find that this is the case.

We have summarized our principal findings diagrammatically in Figs. 10(a)–(c). Fig. 10(a) shows on the left, a possible position for I and I^*, with, on the right, the consequent singularities associated with each, with the sheet specified. Figures 10(b) and 10(c) complete the possibilities for positions of I and I^*. Further sheets, and the singularities in them, can be searched in the same way.

The most significant singularity, physically, is that in $Q(w_-)$ when I is in u_-. We now turn to the question of how effects due to it may be calculated.

5.4. Calculation of Effects due to a Resonance Singularity in s

Following the general method of Sec. 3.4, we make manipulations similar to those leading to the separation given by Eq. (4.11), so that we are left with the problem of calculating $f(s,W^2|I^2)$, this giving the dominant contribution to F_Q in the region of interest.

This problem has been treated in some detail by one of us,[18] and will not be dwelt on here.[19] f is calculated from a dispersion relation in s, the spectral function $[f(s,W^2|I^2)]$, in the notation of Eq. (3.5), being the continuation in λ^2 of the usual one. The example considered in Ref. 18, is, in fact, an unequal mass problem: The reaction is $\pi+N\to\pi+\pi+N$, and the diagram calculated is shown in Fig. 11. The intermediate state is

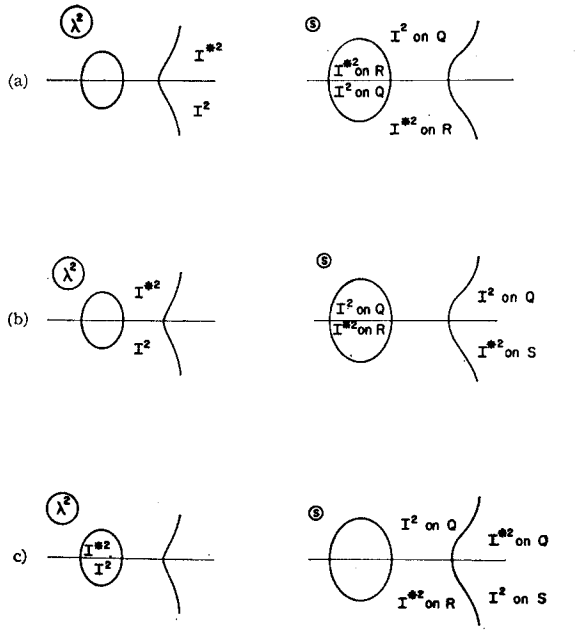

FIG. 10. Summary of results for the crossed channel case of the triangle $F(s,W^2)$. In each of the three cases (a), (b), (c), the left-hand figure shows a possidle location of the σ poles at $\lambda^2=I^2$ and $\lambda^2=I^{*2}$ in the λ^2 plane, while the right-hand figure shows in which sectors of the s plane the related triangle singularities will occur, and on what sheet.

[17] J. Challifour, private communication to P. V. Landshoff quoted in Nuovo Cimento 28, 123 (1963).

[18] I. J. R. Aitchison, Phys. Rev. 133, B1257 (1964), following paper; but see also J. Bronzan, M.I.T. preprint (unpublished).

[19] This graph has also been calculated by S. F. Tuan and T. T. Wu (private communication). Somewhat similar types of graph have been calculated approximately by F. R. Halpern and H. L. Watson (to be published).

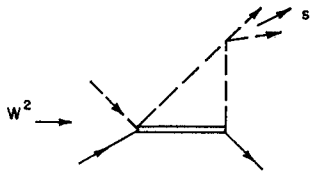

FIG. 11. The process calculated in Ref. 18; the dashed lines are pions, solid lines nucleons, and the double line is the (3,3) isobar.

a pion and the (3,3) nucleon isobar. It turns out that the calculation is sensitive to the actual isobar width, in that the resonance singularity, whenever it is in $Q(w_-)$, is very near the threshold $s=4$. Hence, it is somewhat suppressed. For a very sharp resonance, the calculation shows that the effect produced would be a pronounced peak in $|F|^2$ near $s=4$: that is, at the low mass end of the pion-pion spectrum. Naturally, the singularity is in the critical region $Q(w_-)$ only for a certain range of W; as W is increased, it passes out of $Q(w_-)$ into $Q(w_+)$, passing to the left of $s=4$, and the effect disappears. It is unfortunate that, when it occurs, it is so near $s=4$ that detection of it may prove hard.

We now proceed to our last example, the triangle graph in the direct channel. Here we shall find a similar effect, and it may be physically more interesting.

6. THE TRIANGLE GRAPH WITH A RESONANCE IN THE DIRECT CHANNEL

We once again consider the properties of

$$F(s,W^2)=\frac{1}{\pi}\int_4^\infty d\lambda^2\sigma(\lambda^2)f(s,W^2|\lambda^2), \qquad (6.1)$$

but now as a function of the complex variable W^2, for fixed real $s\geq 4$. The properties of $f(s,W^2|\lambda^2)$ in the two complex variables (W^2,λ^2) have to be determined on the sheets defined by the lower order contractions singularities. One of these, in particular, is the singularity surface $W^2=(\lambda+1)^2$ as found in Sec. 4.2, or Appendix A; that is, (W^2 is a direct variable) the contraction physical sheet is not a simple topological product of two cut planes. Hence, our normal procedure, based on what would, in this case, be a λ^2—W^2 analysis of $f(s,W^2|\lambda^2)$ for fixed s, is much more involved. Therefore we only attempt to find the *nearest* singularities of F instead, and do not give a general method for studying all sheets. We do find a second-sheet resonance (triangle) singularity for F, not to be confused with the resonance (contraction threshold) singularity at $(I+1)^2$. As usual the effect of this can be expressed in terms of $f(s,W^2|I^2)$. While $f(s,W^2|I^2)$ can presumably be evaluated in terms of a dispersion integral along a complex W^2 contour starting at $W^2=(I+1)^2$, a more straightforward, though somewhat circular method, is to use the dispersion relation in s to calculate f for a range of "fixed" physical W^2, and hence the resonance enhancement effect on $F(s,W^2)$, as a function W^2. F will have two resonance peaks, one arising from the complex normal threshold $(I+1)^2$ (woolly cusp), and another from the resonance triangle singularity, both being calculable simply from f. A numerical evaluation of $f(s,W^2|I^2)$ has been performed,[18] and as a function of W^2 the two resonance peaks are distinct, for a sufficiently narrow resonance.

We now describe the method to be used. First, we must define the W^2 physical sheet. For any real $\lambda^2>4$, it is known (see, for example, Ref. 11), that there are no complex singularities of f for any s or W^2 on the physical sheet, there being only an s cut from 4 to ∞, and a W^2 cut from $(\lambda+1)^2$ to ∞. Using this information in (6.1), with an *undistorted* λ^2 contour, we see that $F(s,W^2)$ has as physical sheet the topological product of a $4\leq s<\infty$ cut and a $9\leq W^2<\infty$ cut (as in Sec. 4.2), there being no complex W^2 singularities on the physical W^2 sheet.

Thus we must look to the second and higher W^2 sheets of $F(s,W^2)$ for resonance singularities. We only search the nearest such sheet, reached by continuing W^2 clockwise from above and through its cut, on which from Sec. 4.2, we already know that we will find the singularity $W^2=(I+1)^2$.

We look for effects of the I^2 pole, ignoring those from I^{*2} since we know that the contraction singularity $W^2=(I^*+1)^2$ is fairly far from the physical region; the triangle singularities arising from I^{*2} will be further away. We hence investigate the candidates $W_\pm^2(s,I^2)$ on the physical and nearest unphysical sheet, using the search method [here $W_\pm^2(s,I^2)$ are the two W^2 roots of $\Gamma(s,W^2,I^2)=0$]. That is, we follow a W^2 path to one of $W_\pm^2$, and observe how the λ^2 singularities of f force us to distort the λ^2 contour. The *motion* of these points, $\lambda_\pm^2(s,W^2)$, can be derived from the W^2, λ^2 section of the surface P. However, to avoid facing the problem of the definition of the (W^2,λ^2) physical sheet with respect to $W^2=(\lambda+1)^2$, we determine the *singularity character* of $\lambda_\pm^2(s,W^2)$ by first of all taking W^2 to be real, and using the (s,λ^2) analysis of Appendix B with s real >4; we then preserve the character of each of $\lambda_\pm^2$ as singular or nonsingular when we continue to complex W^2.

The (W^2,λ^2) real section of Γ is shown in Fig. 12, drawn for $4<s<16$. The dashed curve in the same figure is

$$\Delta\equiv[W^2-(\lambda-1)^2][W^2-(\lambda+1)^2]=0, \qquad (6.2)$$

being the contraction singularity surface, singular for $W^2=(\lambda+1)^2$. The points in Fig. 12 are labeled by the same letters as in Fig. 18, for corresponding points, there being two points at infinity on the upper branch of the hyperbola Γ, called a_1 and a_2, corresponding to the one point a of Fig. 18. (Fig. 12 is discussed in more detail in Ref. 11; recall the $s\rightleftarrows\lambda^2$ symmetry of Γ). A point on the arc bc of Fig. 18 corresponds to one on the same-named arc of Fig. 12, etc., with $ab=a_1b$, $ae=a_2e$.

In the (s,λ^2) treatment, Appendix B, for *real* W^2, the physical s limit was $s+i\epsilon$. For ϵ nonzero, $\lambda_\pm^2$ then also has imaginary parts whose sign can be real off Fig. 18 (which gives $d\lambda^2/ds$). Further, we know from Appendix B

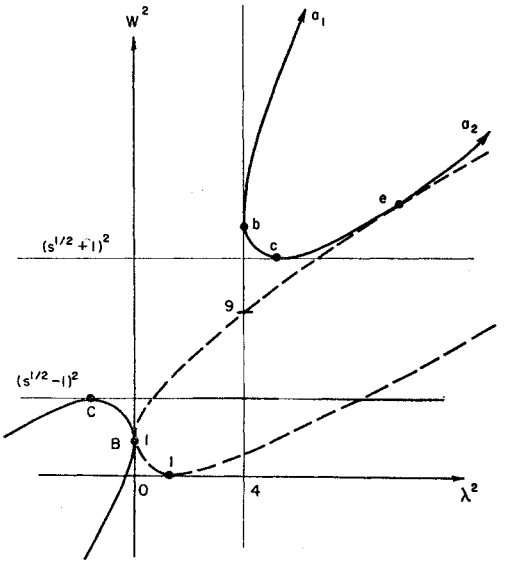

FIG. 12. The real (W^2,λ^2) section of $\Gamma(s,W^2,\lambda^2)$, for real $s>4$; also that of $\Delta\equiv[W^2-(\lambda+1)^2][W^2-(\lambda-1)^2]=0$ (broken curve). The various points shown are at: b, $W=2s+1$; c, $\lambda^2=W+1=s^{1/2}+2$; e, $W^2=(s-1)^2$, $\lambda^2=(s-2)^2=(W-1)^2$; C, $\lambda^2=-W+1=-s^{1/2}+2$.

whether each of $\lambda_\pm^2$ is singular or nonsingular on the *physical* λ^2 sheet with this imaginary part. However, what we will really want to know is the singularity character of each of λ_+^2 and λ_-^2 when reached on the two paths in the λ^2 plane, on the physical sheet starting to the right of the branch point $\lambda^2=(W-1)^2$, which circle to the λ^2 under consideration in a clockwise and in an anticlockwise sense with respect to this branch point. Recall that the location of the cut is arbitrary, and the language of paths is more appropriate for a function on a Riemann surface than that of cuts. We call these path senses clockwise and anticlockwise.

Since each of $\lambda_\pm^2$ is singular on one but not the other of the two sheets of $f(s,W^2|\lambda^2)$ with respect to $\lambda^2=(W-1)^2$, we can easily determine the answer. When we turn to (W^2,λ^2) and Fig. 12 we commence with s real >4, and W^2 on its physical side of its cut from 9 to ∞, i.e., $W^2+i\epsilon$. We again find a definite sign of the imaginary part of λ_+^2 and λ_-^2, but this sign will not always be the same as that given by the (s,λ^2) method. However, the λ^2 cut will be displaced slightly into the upper half-plane due to the displacement of its end point $\lambda^2=(W-1)^2$, and in fact the singularity character on the clockwise and anticlockwise paths must necessarily be the same as found by (s,λ^2). (Both $s+i\epsilon$ and $W^2+i\epsilon$ give the same *physical* limit of the physical sheet.) We therefore get the starting characters as shown in Table I. We see that the sense in which λ^2 is singular changes at e, the contact of Γ with the lower order singular contraction Δ.

Let us consider an s which is only slightly larger than 4, specifically $(s-2)^2\ll \mathrm{Re}I^2$. We commence with $W^2+i\epsilon$ on its physical sheet with $W^2\gg(s-1)^2$ and the two λ^2 singularities of $f(s,W^2|\lambda^2)$ on the branches $a_1b(\lambda_-^2)$ and $ea_2(\lambda_+^2)$. The λ^2 contour is then as shown in Fig. 13(a); here each of $(W-1)^2$, λ_-^2 and λ_+^2 has a small positive imaginary part, the λ^2 integration goes along the real axis, and in order to display the clockwise sense of $\lambda_\pm^2$, we have slightly deformed the λ^2 cut upwards.

TABLE I. The starting point of the direct channel analysis: The singularity characters are transferred from the crossed channel case.

	(s,λ^2) $\mathrm{Im}\lambda^2$	Singular on p sheet	Singular in which sense	(W^2,λ^2) $\mathrm{Im}\lambda^2$
a_1b	−	no	anticlockwise	+
bc	+	yes	anticlockwise	−
ce	−	no	anticlockwise	+
ea_2	+	no	clockwise	+

Let W^2 move on a fairly direct path into the lower half-plane through the W^2 cut, towards $W^2=(I+1)^2$. We then obtain the situation shown in Fig. 13(b). All three of λ_-^2, λ_+^2 and $(W-1)^2$ have moved into the lower half of the λ^2 plane, to the right of $\lambda^2=4$; however, they have not changed their relative locations. Both λ_+^2 and $(W-1)^2$ are singular, and cause the λ^2 contour to be moved downwards. At $W^2=(I+1)^2$ we see that the λ^2 contour is pinched between the pole of σ at $\lambda^2=I^2$ and the contraction singularity $\lambda^2=(W-1)^2$ so that $W^2=(I+1)^2$ is a singularity of F on Q. This is nothing more than the singularity of the three-particle intermediate state two-particle amplitude discussed in Sec. 4.2.

Now consider, instead, a W^2 path which goes towards $W_-^2(s,I^2)$, passing in a clockwise sense around $W^2(I+1)^2$. Here $W_-^2(s,I^2)$ is that W^2 root of $\Gamma(s,W^2,I^2)=0$ for which $\lambda_+^2(W_-^2)=I^2$; and similarly $W_+^2(s,I^2)$ is defined by $\lambda_-^2(W_+^2)=I^2$. (Note that for I^2 real >4, $\lambda_+^2>\lambda_-^2$, $W_+^2>W_-^2$, all being real.) We

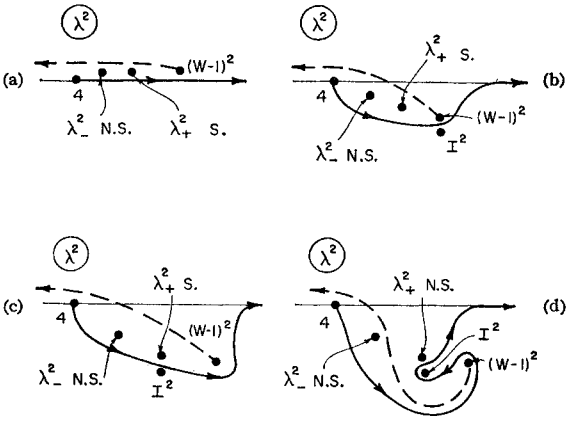

FIG. 13. The λ^2 contour and cut (dashed) of $F(s,W^2)$, for various W^2; (a) W^2 real, on physical edge of physical sheet P; (b) $W^2=(I+1)^2$ on Q; (c) $W^2=W_-^2(I^2)$ on Q, for W^2 passing clockwise about $(I+1)^2$; (d) as in (c), but W^2 passing $(I+1)^2$ anticlockwise.

then get the situation shown in Fig. 13(c). The λ^2 contour is between I^2 and $\lambda_-{}^2$, and at this point $f(s,W^2|\lambda^2)$ is being seen in a clockwise sense with respect to $(W-1)^2$, so that $\lambda_-{}^2$ is singular. Hence, on a clockwise W^2 path to $W_-{}^2$, $W_-{}^2$ is a singularity of $F_Q(s,W^2)$.

On the other hand, if the W^2 path to $W_-{}^2$ had passed around $W^2=(I+1)^2$ in an anticlockwise sense, we would have found the situation of Fig. 13(d). Now the $\lambda^2\approx I^2$ part of the λ^2 contour is seen in an anticlockwise sense with respect to $\lambda^2=(W-1)^2$; for this sense $\lambda_-{}^2$ is not singular, so that the "pinching" shown in Fig. 13(d) is only apparent. In an anticlockwise sense $W_-{}^2$ is not a singularity of $F_Q(s,W^2)$. [We should point out that we are free to move the λ^2 cut as we wish, since only the sense of a point is significant. Thus between Fig. 13(c) and Fig. 13(d) $\lambda_-{}^2$ has crossed the cut; however, it has never crossed the contour when in a singular sense. In general, for a given sense any $\lambda_\pm{}^2$ point may cross the λ^2 contour if it is nonsingular but must push the contour ahead of itself if it is singular.]

We use precisely similar methods to show that $W_+{}^2(s,I^2)$ is a singularity of $F_Q(s,W^2)$ if reached in an anticlockwise sense about $W^2(I+1)^2$, but is nonsingular in a clockwise sense. In summary,

$$\begin{aligned} &W_-{}^2(s,I^2) \text{ singular in clockwise sense,}\\ &\qquad\qquad\qquad\qquad \text{not anticlockwise.}\\ &W_+{}^2(s,I^2) \text{ singular in anticlockwise sense,}\\ &\qquad\qquad\qquad\qquad \text{not clockwise.} \end{aligned} \tag{6.3}$$

It will be seen that the different conclusions for $W_-{}^2$ and $W_+{}^2$ arise because $\lambda_+{}^2\in ea_2$ is singular in a clockwise sense, but $\lambda_-{}^2\in a, b$ is singular in an anticlockwise sense (cf. Table I). It may well be asked what happens if we leave P for Q at a $W^2<(s-1)^2$, so that $\lambda_+{}^2\in ce$, and is now nonsingular in a clockwise sense. Apparently $W^2=(s-1)^2$ is a first-sheet singularity of F in the physical region. A little thought shows that this is not the case. $W^2=(s-1)^2$ is a special point of the mapping, and near it we find

$$[\lambda_-{}^2-(W-1)^2]\propto -[W^2-(s-1)^2]^2;$$

as W^2 circles the point $W^2=(s-1)^2$ once, $\lambda_-{}^2$ makes two complete revolutions with respect to the $\lambda^2=(W-1)^2$ branch point. This is true regardless of the size of the W^2 closed path enclosing $(s-1)^2$. It then can be shown that we reach the *same* conclusions, Eq. (6.3), regardless of where we start with W^2. In fact, we can start with any $W^2>9$, independently of s, with W^2 real and the two $\lambda_\pm{}^2$ being complex conjugate on the surface *BCbc*. Our initial restriction that $(s-2)^2\ll \mathrm{Re}I^2$ is also irrelevant to the final conclusions. It was made to ensure that in Fig. 13(a–d), no violent gyrations of relative positions would occur. It is straightforward to follow the λ^2 contour and singularities for many different W^2 paths; however, the various domains in the W^2 plane do not have any particularly direct physical significance.

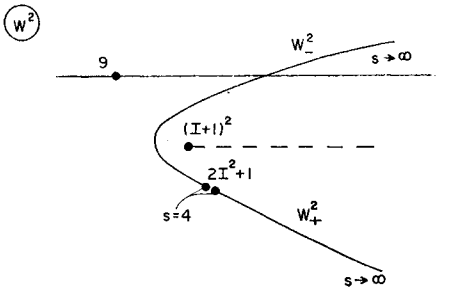

FIG. 14. The motion of $W_\pm{}^2(s,I^2)$ in the complex W^2 plane, for s moving along the real axis from 4 to ∞. The cut starting at $W^2=(I+1)^2$ is also shown.

There are many other sheets which could be investigated, and among other singularity candidates are $W^2=(\lambda_0-1)^2=1$ (the nonsingular pseudonormal threshold), and the second type singularities $W^2=(s^{1/2}+1)^2$ and $W^2=(s^{1/2}-1)^2$. The latter are *not* singular on the physical edge of P. Thus all other candidates are further away from P than those we have found in Eq. (6.3).

We show the location of $W_\pm{}^2(s,I^2)$ for all $s\geq 4$ in Fig. 14. The curve is one branch of a hyperbola. The important features are that $W_+{}^2=W_-{}^2=2I^2+1$ for $s=4$; as s increases, $W_+{}^2$ moves down and to the right, while $W_-{}^2$ circles to the *left* of $(I+1)^2$, and ultimately crosses the real W^2 axis. These properties can be obtained directly from the form $\Gamma(s,W_\pm{}^2,I^2)=0$, or, more neatly, by rewriting $\Gamma=0$ in terms of the familiar external variables[20] x, y, and z defined by $W^2=1+I^2-2Ix$, $s=2(1-y)$, $\frac{1}{2}I=z$. $\Gamma=0$ then becomes $x^2+y^2+z^2-2xyz-1=0$, and the mapping of the real y axis in Γ is a degenerate quartic[21] made up of an ellipse and a hyperbola. The real s axis with $s\geq 4$ maps into one branch of the hyperbola.

The properties Eq. (6.3) apply for all real $s\geq 4$. The reason for our initial restriction $(s-2)^2\ll \mathrm{Re}I^2$ was to ensure that $W_-{}^2$ had not yet circled $W^2=(I+1)^2$, for at this moment the $\lambda_\pm{}^2$ also starts gyrations relative to $\lambda^2=(W-1)^2$, which would have led to unnecessary confusion.

The result Eq. (6.3), as regards $W_+{}^2$, implies that $W_+{}^2$ is only singular if W^2 moves on Q along a path which avoids the $W^2=(I+1)^2$ cut shown in Fig. 14. Thus, the *singularity* $W_+{}^2$ is always rather far from the physical region. $W_-{}^2$ is not singular on a clockwise path with respect to $W^2=(I+1)^2$. For small $s>4$ anticlockwise clearly means on a path which avoids the $W^2=(I+1)^2$ cut, and as s increases *this* definition cannot change, even though the word anticlockwise is hardly appropriate by the time $W_-{}^2$ has entered the upper half-plane. Similarly "clockwise" means on a W^2 path which leaves Q through the upper edge of the $(I+1)^2$ cut, to

[20] R. Karplus, C. M. Sommerfield, and E. D. Wichmann, Phys. Rev. **111**, 1187 (1958).

[21] G. Bonnevay, I. J. R. Aitchison, and J. S. Dowker, Nuovo Cimento, **21**, 1001 (1961).

another sheet R. On this sheet W_-^2 *is* singular. It is also singular on the sheet R' reached by leaving Q through the lower edge of the $W^2=(I+1)^2$ cut, as can be verified by following such a W^2 path for small s. It is customarily asserted that $W^2=(I+1)^2$ is a square-root branch point. We have not been able to prove this by our methods, but have found no contradiction; that is, $R'\equiv R$ is very plausible.

In terms of these sheets, our final conclusions for $F(s,W^2)$ are:

$$\begin{aligned}&\text{(i)}\quad W^2=(I+1)^2, \quad \text{singular on } Q;\\ &\text{(ii)}\quad W^2=W_+^2(s,I^2), \quad \text{singular on } Q, \text{ not on } R;\\ &\text{(iii)}\quad W^2=W_-^2(s,I^2), \quad \text{singular on } R, R', \text{ not on } Q;\end{aligned} \tag{6.4}$$

when $\mathrm{Im}W_-^2>0$, Q becomes P, not singular.

We now ask if any of these are likely to have observable effects.[22] The threshold $W^2=(I+1)^2$ will, of course, lead to a woolly cusp effect, exactly as for the scattering amplitude of Sec. 4.2. W_+^2 is always far away from the physical sheet, so will never have an effect. However, for sufficiently small $s>4$, W_-^2 can have an effect, since then the path from the upper edge of the $(I+1)^2$ threshold cut into R will be fairly short. This is especially the case if $|\mathrm{Im}I^2|\ll\mathrm{Re}I^2$, for then Fig. 12 becomes contracted in the vertical scale. Thus, for a sufficiently narrow resonance, and for sufficiently small (fixed) $s>4$, $F(s,W^2)$ should show two separate resonance "peaks," one associated with $W^2=(I+1)^2$ and the other with the resonance triangle singularity $W_-^2(s,I^2)$.

As usual, these enhancements can be calculated by explicitly separating out the resonance contribution, i.e.,

$$F(s,W^2)=\hat{F}(s,W^2)-2iR(I^2)f(s,W^2|I^2). \tag{6.5}$$

We do not discuss the question of evaluating discontinuities in detail. From Eq. (6.5) it is clear that the essential properties of F_Q are given by $f(s,W^2|I^2)$. If we write a dispersion relation in W^2 for $F_P(s,W^2)$, with contour the real W^2 axis from 9 to ∞, this contour can be swung down into the lower half W^2 plane, revealing the beginning of the sheet Q. Then, as shown in Fig. 15, if we swing down sufficiently far and around, we can write two separate contour integrals. It seems clear that the integration along C_1 will give $\hat{F}$, while that around C_2 will give the separate contribution from the resonance $f(s,W^2|I^2)$. Since W^2 is a direct variable, C_2 encloses *two* singularities, the contraction threshold and also the triangle singularity W_+^2. The sum of these contributions will give $f(s,W^2|I^2)$. However, since ultimately we will want to take both s and W^2 real and physical, there is a much easier way of evaluating f, namely by use of an

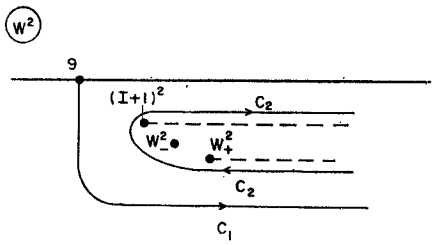

FIG. 15. The distorted W^2 dispersion integral path for $F(s,W^2)$. The part C_1 gives $\hat{F}$, with no resonance singularities near the physical edge of P; while C_2 leads to the explicit separation of the resonance contribution $f(s,W^2|I^2)$.

s dispersion relation, for which there is *only one* branch point. This is exactly the same calculation as discussed in Sec. 5.4. When $f(s,W^2|I^2)$ is evaluated numerically,[18] one does actually find that for a sufficiently narrow resonance, f shows two *resolved* "peaks" in W^2 for fixed s very close to threshold $s=4$; of the two peaks one is due to the woolly cusp singularity $W^2=(I+1)^2$; the other is due to the triangle resonance singularity at $W_-^2(s,I^2)$. The significance of this result is discussed further in Ref. 18.

7. SUMMARY AND CONCLUSIONS

We now review the techniques we have used and comment on the results we have obtained. The basic problem considered was the meaning and application of a perturbation theory graph when it contains an internal particle of complex mass. We stated with an arbitrary graph F in which the full two-particle Green's function (or propagator) G was inserted between two points (the resulting graph being then, in fact, a sum of many Feynman graphs).

We wrote F (cf. Sec. 2) as an integral of the product of the spectral function σ of G and the Feynman graph $f(|\lambda^2)$ obtained from F by replacing G with a single line of mass λ, the integral being over λ^2. We considered the case in which G had a resonance, corresponding to poles of σ at $\lambda^2=I^2$ and I^{*2}. Then F could be written, quite generally, as the sum of $f(|I^2)$ and another "background" term coming from the continuum part of G, not the pole.

Within this framework we attempted to answer three questions. First, what are the analytic properties of F, given such a resonance structure in G? Second, under what conditions are these properties sufficiently similar to those of $f(|I^2)$ that the latter is a good approximation to F? Third, what observable effects are expected from singularities associated specifically with the resonance, and how may they be calculated?

To answer the first question, the singularities of the λ^2 integral representation for F had to be analyzed and this necessitated a prior analysis of the perturbation theory graph $f(|\lambda^2)$ as a function of the *internal* mass λ^2. Three examples were considered in detail. By way of introduction, the first, a trivial one, was the two-particle

[22] In what seems to be the first consideration of resonances as internal lines, a triangle with a resonance in the direct channel (in this case the s channel) was calculated approximately by R. Aaron, Phys. Rev. Letters **10**, 32 (1963). However, there the interest was rather different.

scattering amplitude with two-particle intermediate states as a function of the energy variable W^2. Apart from inessential factors, this amplitude is just G itself and $f(|\lambda^2)$ is $1/(W^2-\lambda^2)$. We rederived the well-known result that the poles in σ reappear as second-sheet poles of G. Of these, the one at $W^2=I^2$ may be near the physical region, and if so, it leads to an enhancement effect in G. Our techniques show why $f(|I^2)$ is a suitable approximation to G for calculating this enhancement, while, on the other hand, $f(|I^{*2})$, *a priori* an equally plausible candidate, is not.

A less trivial example was that of the two-particle amplitude with three-particle intermediate states, $F(W^2)$, one pair of the particles interacting via G. Here $f(|\lambda^2)$ was the single-loop self-energy function, and was analyzed in detail in Appendix A. The analysis of $F(W^2)$ was done in Sec. 4, and the singularities of F associated with the resonance in G were found. Of physical significance was a square-root branch point on an unphysical sheet near the physical region, closely analogous to the resonance pole of the first example. We showed that the effect of this branch point in F could be calculated correctly by evaluating $f(|I^2)$.

Our main example was the triangle graph $F(s,W^2)$, as a function of each of two external invariants s and W^2. $f(|\lambda^2)$ for this case was discussed in Appendix B, and the properties of F were given in Secs. 5 and 6. Two singularities of F appeared to be of special physical significance. First, as a function of s, F could have a logarithmic branch point on an unphysical sheet near the physical region, for a certain range of W^2. Second, F could have an analogous branch point in W^2 for a certain range of s. In the first case, we showed that effects due to this branch point could again be calculated by evaluating $f(|I^2)$, and the prescription for doing this was given. However, we were not able to carry through the analogous calculation in the second case, and we had to resort instead to the first prescription, evaluated for a given fixed s and many values of W^2, thereby calculating $F(s,W^2)$ along the real W^2 axis. These calculations, reported elsewhere,[18] indicate that if the width of the resonance is small, effects due to these "resonance singularities" may be observable.

From these three examples we draw the following conclusions. In a certain range of the energy variable W^2, the two-particle scattering amplitudes may be well approximated by any simple form which represents a pole in W^2, near the physical region. Correspondingly, more complicated graphs F containing the two-particle propagator G internally may be approximated, in certain energy ranges, by simply replacing G with a complex pole, that is, by a graph $f(|I^2)$ which has an internal particle of complex mass. Although, in general, the singularities of $f(|I^2)$ and F are quite different, for these energy ranges two necessary requirements hold: firstly, only certain singularities of F associated with the I^2 pole in G ("resonance singularities") need be considered, and secondly, these singularities of F are contained in f. In that case, the "background" part of F—which we are unable to calculate—does not cancel these singularities, so that we are justified in calculating their effect from $f(|I^2)$. We conjecture that whenever a calculation of $f(|I^2)$ shows an effect in the physical region due to a resonance singularity, it is a legitimate approximation to F, but not otherwise; this is, after all, quite satisfactory. In the examples considered, $f(|I^{*2})$ is never a good approximation.

ACKNOWLEDGMENTS

This work was carried out during the summer of 1963. One of us (C. K.) is very grateful to Dr. G. C. Wick for his hospitality at Brookhaven during this period.

APPENDIX A: PROPERTIES OF $f(W^2|\lambda^2)$

Following standard methods[23] one has

$$f(W^2|\lambda^2)=\int_0^1 d\alpha_1\int_0^1 d\alpha_2\delta(\alpha_1+\alpha_2-1)\ln\Lambda, \quad \text{(A1)}$$

where

$$\Lambda=\alpha_1+\alpha_2\lambda^2-\alpha_1\alpha_2W^2-i\epsilon=\alpha Z\alpha, \quad \text{(A2)}$$

Z being the 2×2 matrix

$$Z=\begin{bmatrix} 1 & \frac{1}{2}(1+\lambda^2-W^2) \\ \frac{1}{2}(1+\lambda^2-W^2) & \lambda^2 \end{bmatrix}. \quad \text{(A3)}$$

Since λ^2 is one of the variables, we have not performed the usual transformation on the α_i which makes $z_{ii}=1$ (c.f. Ref. 20). We now enumerate the possible singularity surfaces.

(i) $\alpha_1=0$, $\alpha_2=1$ end point. This gives $\Lambda=0$ if $\lambda^2=0$ so that there is a singularity surface $\lambda^2=0$; but see (iv).

(ii) $\alpha_1=1,\alpha_2=0$ end point. Similarly this gives $\lambda^2=\infty$.

(iii) α_1 coincident singularities. This gives the parabola

$$\Sigma\equiv\det Z\equiv[W^2-(\lambda+1)^2][W^2-(\lambda-1)^2]$$
$$\equiv[\lambda^2-(W+1)^2][\lambda^2-(W-1)^2]=0. \quad \text{(A4)}$$

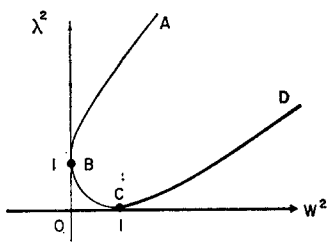

FIG. 16. The real (W^2,λ^2) section of the various singularity surfaces of the single-loop self-energy function $f(W^2|\lambda^2)$. The heavy lines are singular on the physical sheet.

[23] R. J. Eden, Maryland Physics Department Report No. 211, 1961 (unpublished), especially p. II, 4 ff. We are ignoring a subtraction term needed for convergence since it is independent of W^2.

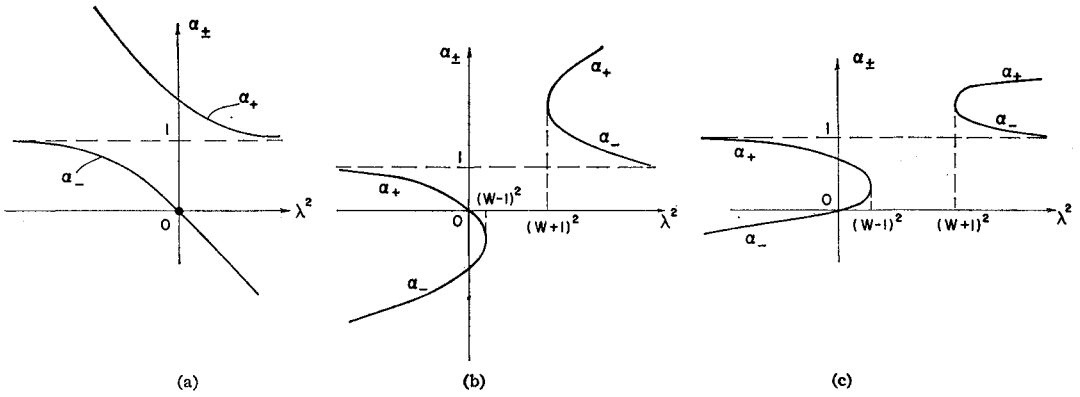

FIG. 17. The location of the Feynman denominator α singularities $\alpha_\pm$ of $f(W^2|\lambda^2)$ for real λ^2 for the three cases (a) $W^2<0$; (b) $0<W^2<1$; and (c) $1<W^2$.

For real W^2 and λ^2, we see that $\alpha_1/\alpha_2=-\frac{1}{2}(1+\lambda^2-W^2)$, which implies $0<\alpha_1,\alpha_2<1$ for $W^2=(1+\lambda)^2$, i.e., $\lambda^2=(W-1)^2$ with $W^2\geq 1$; but α_2 outside 0 to 1 otherwise.

(iv) Another possible singularity is $W^2=\infty$, which actually comes under both types (i) and (ii), but is easy to overlook. For $W^2\to\infty$, λ^2 finite, one has $\alpha_1\sim\lambda^2/W^2$ or $\alpha_1\sim 1+1/W^2$. Thus, as W^2 does a circle about the point at infinity, the two α_1 singularities circle synchronously about the two α_1 end points 0 and 1.

(v) Finally we must include the possible second type singularity[12] $W^2=0$. We show the real sections of these surfaces in Fig. 16. By inspection of Eq. (A4), Λ never vanishes on the undistorted α_i region of integration if $\lambda^2>0$ and $W^2<0$; nor if $\mathrm{Im}\lambda^2<0$, $\mathrm{Im}W^2>0$, this being the definition of the physical limit. Hence, end point contraction cuts should be taken along the whole of the negative real λ^2 axis (we postpone discussion of $W^2=\infty$). Turning to the coincident singularities, the complete real section of Σ can be reached from the physical limit (with undistorted α_i paths), and thus we see that only the branch CD is singular (since for it the pinch occurs between 0 and 1). The W^2 branch cut runs from $W^2=(\lambda+1)^2$ to $W^2=\infty$; the possible second type singularity $W^2=0$ is, therefore, not singular on the physical sheet. A remark important for the analysis of Sec. 4.2 is that the complex extension of Σ is singular only from CD. We see that following $ABCD$ the singularity character changes only at C, at contact with a singular lower order curve, but not at B, exactly as in more standard analyses.

An unusual feature is that $\lambda^2=0$ is always a singularity, as well as $\lambda^2=(W-1)^2$ for $W^2\geq 1$. This can be seen in more detail if we solve for the α_i. We eliminate α_2, then

$$\Lambda=W^2\alpha_1^2+\alpha_1(1-\lambda^2-W^2)+\lambda^2-i\epsilon$$
$$=W^2(\alpha_1-\alpha_+)(\alpha_1-\alpha_-),$$

with $\alpha_\pm=[(\lambda^2+W^2-1)\pm\Sigma^{\frac{1}{2}}]/2s$. We show $\alpha_\pm$ versus real λ^2 in Fig. 17(a) for $W^2<0$, Fig. 17(b) for $0<W^2<1$, and Fig. 17(c) for $1<W^2$ (most easily obtained by solving $\Lambda=0$ for λ^2 in terms of α_1). From Fig. 17 we see that for $W^2<1$ there is one (and only one) α_1 singularity on the undistorted α_1 contour for $\lambda^2<0$, and none for $\lambda^2>0$; while for $W^2>1$ there is one α_1 singularity for $\lambda^2<0$, but two for $0<\lambda^2<(W-1)^2$, these being coincident at $\lambda^2=(W-1)^2$. Hence $\lambda^2=0$ is always a physical sheet branch point, as is $\lambda^2=(W-1)^2$ for $W^2>1$. By explicitly performing the α_1 integration one easily sees that the latter is two sheeted; however, the former is actually a logarithmic singularity, with

$$f\approx\frac{-\lambda^2}{W^2-1}\left[\ln\left(\frac{-\lambda^2}{W^2-1}\right)-1\right]$$

for $W^2\neq 1$, $\lambda^2\approx 0$.

APPENDIX B: PROPERTIES OF THE TRIANGLE GRAPH, $f(s,W^2|\lambda^2)$, FOR COMPLEX s AND λ^2

We now turn to the properties of the triangle graph [Fig. 3(b)] in perturbation theory. This has been studied by Bronzan and one of the present authors (C. K.)[11] in terms of s and λ^2, for fixed real $W^2>9$. We briefly summarize their findings.

The physical sheet for $f(s,W^2|\lambda^2)$ is defined with respect to the various contraction singularities. In s the contractions give rise to the usual normal threshold cut running along the real s axis from 4 to ∞, the physical limit being from above. ($s=0$ is a branch point on the second contraction sheet reached by going through the normal cut.) The other contraction leads immediately to the self-energy function $f(W^2|\lambda^2)$, which has been treated in Appendix A. From $f(W^2|\lambda^2)$ one has, for $W^2>9$, two independent inverse square root λ^2 cuts along the real axis, one from $-\infty$ to 0 and one from $-\infty$ to $(W-1)^2$, the physical limit being from below each of these cuts. The (leading) singularity surface is

$$\Gamma(s,W^2,\lambda^2)\equiv s\lambda^2(s+\lambda^2-W^2-3)+(W^2-1)^2=0. \quad \text{(B1)}$$

Finally we have possible second type singularities on

$$\Sigma(s,W^2)\equiv[s-(W+1)^2][s-(W-1)^2]=0. \quad \text{(B2)}$$

The real section of the surface Γ is shown in Fig. 18, in which capital and lower case letters are paired by the links of the complex surfaces.

As well as the physical sheet of f, on which it is denoted by f_{pp}, we have the various sheets obtained by continuing *through* one or more of the contraction cuts arising from the branch points $s=4$, $\lambda^2=0$ and $\lambda^2=(W-1)^2$. In particular, we will be interested in the properties of f_{qp} and f_{pq}, where the second suffix q denotes λ^2 on the second sheet of the $\lambda^2=(W-1)^2$ cut, reached by *avoiding* the $\lambda^2=0$ cut (recall all these cuts are two sheeted).

For a given s, there are always two λ^2 points on Γ, and the properties of f on the various sheets are fully determined once we know for which sheets these λ^2 points are in fact singular. If a given point (s,λ^2) is singular (nonsingular) for f_{pp}, then it is nonsingular (singular) for f_{qp} and f_{pq}, etc. This is a straightforward generalization of Theorem 3.2 of Ref. 10.

Consider now an s moving continuously from slightly above the normal cut on p to slightly below this cut on q, with $4\leq \mathrm{Re}(s)\leq(W-1)^2$; then the two λ^2 points will also move continuously, and each will cross the λ^2 cut between 4 and $(W-1)^2$. The character of each of the λ^2 points remains fixed as long as we do not jump across a cut. Let us follow the λ^2 root of Γ which has an infinitesimal imaginary part of the same sign as that of s; then the singularity character of this point for f_{pp} is the same as that for f_{qq}, and that for f_{pq} is the same as that for f_{qp}. Our restriction to $4<s<(W-1)^2$ is not necessary but was used to ensure avoiding the $\lambda^2=0$ cut.

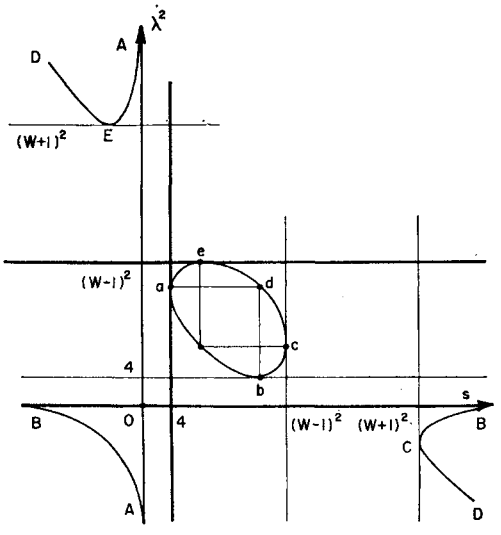

FIG. 18. The real (s,λ^2) section of the various singularity surfaces of the triangle $f(s,W^2|\lambda^2)$ for real $W^2>9$. The heavy lines show *singular* lower order contractions, and the curve is $\Gamma(s,W^2,\lambda^2)$. The various points are at: a, $\lambda^2=\frac{1}{2}(W^2-1)$; b, $s=\frac{1}{2}(W^2-1)$; c, $\lambda^2=W+1$; e, $s=W+1$; c, $\lambda^2=-W+1$; e, $s=-W+1$.

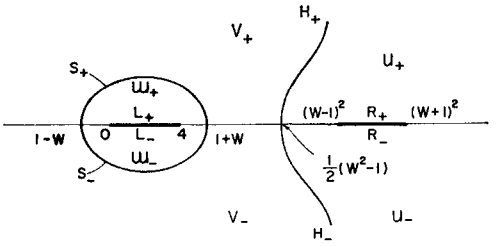

FIG. 19. The various complex plane domains of the mapping $s\rightarrow\lambda_\pm^2(s)$, these being the roots of $\Gamma(s,W^2,\lambda^2)=0$ for real $W^2>9$.

We now state the singularity characters. Recalling that f_{pp} means the function f in the first s and λ^2 sheets, defined with respect to the cuts associated with the singularities $s=4$, $\lambda^2=0$, and $\lambda^2=(W-1)^2$, respectively, we find that f_{pp} has complex singularities on the two complex conjugate branches of the surface $bcBC$, but on no other surface. The second type singularity $s=(W-1)^2$ is singular on the lower (unphysical) edge of the s cut, for $\lambda^2<W+1$; no other singularities exist for f_{pp}. Those on the other sheets can easily be derived from this (but see below).

To study $F(s,W^2)$ we must follow the motion of the λ^2 singularities of $f(s,W^2|\lambda^2)$ as s moves in the complex plane, i.e., we need the motion of the roots $\lambda_\pm^2(s)$ of $\Gamma(s,W^2,\lambda^2)=0$. Figure 18 really contains complete information, but it is useful to give a few more details. A further treatment of the mapping $s\rightarrow\lambda_\pm^2$ has been given elsewhere.[24]

In the equal mass case this mapping is particularly simple, since $\Gamma(s,W^2,\lambda^2)$ is symmetric under $s\rightleftarrows\lambda^2$ (cf. Fig. 18); however the typical features given below are general. Both the s and λ^2 planes can be divided into six regions as shown in Fig. 19, called $u_\pm$, $v_\pm$, and $w_\pm$.

The exact form of the boundary curves is unimportant (but see Ref. 24). The upper and lower halves of the closed curve are called $S_\pm$, and of the "bow" curve $H_\pm$. The mapping is double valued, a given s determines two points λ_+^2 and λ_-^2. "Naming" cuts are introduced for $0\leq s\leq 4$ and $(W-1)^2\leq s\leq(W+1)^2$, called L and R, respectively, with upper and lower edges $L_\pm$ and $R_\pm$. These naming cuts are simply to guarantee that the same point is always given the same name; for example, for $s\epsilon R$, λ_+^2, and λ_-^2 are complex conjugate, with large imaginary parts. We specify $\mathrm{Im}\lambda_\pm^2/\mathrm{Im}s\gtrless 0$. Then as s crosses from R_+ to R_- moving infinitesimally, λ_+^2 and λ_-^2 seem to jump discontinuously, but in fact $\lambda_+^2(s-i\epsilon)$ is infinitesimally close to $\lambda_-^2(s+i\epsilon)$.

One finds that the various domains of Fig. 19 map into each other as follows:

$$\begin{aligned}
\lambda_+^2:\ & u_\pm\rightarrow v_\mp & \lambda_-^2:\ & u_\pm\rightarrow w_\pm\\
& v_\pm\rightarrow u_\mp & & v_\pm\rightarrow w_\mp\\
& w_\pm\rightarrow u_\mp & & w_\pm\rightarrow v_\mp
\end{aligned} \quad \text{(B3)}$$

[24] C. Kacser, Phys. Rev. 132, 2712 (1963).

(where λ_+^2: $u_+ \to v_-$ means $s \in u_+$, $\lambda_+^2(s) \in v_-$). Further, we obtain

$$\begin{array}{lll} \lambda_+^2: & L_\pm \to H_\pm & \lambda_-^2: \quad L_\pm \to H_\mp \\ & R_\pm \to S_\mp & \qquad\quad R_\pm \to S_\pm \\ & H_\pm \to H_\mp & \qquad\quad H_\pm \to L \\ & S_\pm \to R & \qquad\quad S_\pm \to S_\mp . \end{array} \tag{B4}$$

The mapping of other parts of the real s axis can be read off Fig. 18. We have defined $\lambda_\pm^2$ such that $\lambda_+^2 \geq \lambda_-^2$ for real $s<0$ and $4<s<(W-1)^2$, but $\lambda_+^2 \leq \lambda_-^2$ for real $s \geq (W+1)^2$. The curves S and H are in fact defined by the conditions (B4).

After these lengthy preliminaries, the properties of $f(s,W^2|\lambda^2)$ on the nearest sheets can be listed as follows:

$$\begin{array}{lll} \text{(a)} & f_{pp}: & \lambda^2 \text{ singular only if } s \in u_\pm;\ \lambda_+^2 \text{ not singular, } \lambda_-^2 \text{ singular } \in w_\pm^2 \\ \text{(b)} & f_{pq}=f_{qp}: & \text{for } s \in v_\pm,\ w_\pm \text{ both } \lambda_\pm^2 \text{ singular; for } s \in u_\pm,\ \lambda_+^2 \in v_\pm^2 \text{ is singular, } \lambda_-^2 \in w_\pm^2 \text{ not singular.} \end{array} \tag{B5}$$

We remark that for f_{qp}, as s crosses λ_+ from v_+ to u_+, λ_-^2 crosses the λ^2 cut from below between 0 and 4 [cf. (B4)], having been singular on the p sheet in λ^2 for $s \in v_+$. This singularity passes smoothly on the Riemann surface to the q sheet in λ^2 as s enters u_+.

PHYSICAL REVIEW VOLUME 133, NUMBER 5B 9 MARCH 1964

Logarithmic Singularities in Processes with Two Final-State Interactions*

I. J. R. AITCHISON†
Brookhaven National Laboratory, Upton, New York
(Received 7 October 1963)

The effects of logarithmic singularities in rescattering processes are investigated. The reaction $\pi N \to \pi\pi N$ is considered, but treated purely as an S-wave, spinless model. A particular triangle graph is analyzed in detail; it contains as an intermediate state the (3,3) nucleon isobar I, which is described as a spinless particle of complex mass. The graph is calculated from a dispersion relation as a function of the mass s of the two pions in the final state, for low values of the over-all c.m. system energy W. The relation is then analytically continued in W. For a narrow range in W, an enhancement of the square of the amplitude is found near $s=4$ (the pion mass is unity). The analogous enhancement also appears in the W channel near $W=I+1$, for a small range of s only, near $s=4$. The prominence of the effect depends on the width of I, being closely connected with the nearness to the physical region of one of the two logarithmic singularities (anomalous thresholds) of the graph: this distance increases sharply with the isobar width. The positions of the singularities are interpreted as the phase-space limits for the simultaneous production of states with mass s and I. The conclusion is that such a "double excitation" process leads to an enhancement of the triangle amplitude only if, in general, s and I fall in certain narrow ranges. The implications of this result for models of the higher resonances in the elastic channel ($\pi N \to \pi N$) is briefly discussed.

I. INTRODUCTION

UNTIL the rather recent introduction of self-consistent (bootstrap) methods using the N/D formalism,[1] it is fair to say that most calculations of dynamical effects in strong interactions have been single-particle exchange calculations. However, it is worth asking how we may go further, and include rescattering terms, which arise from the fact that in a multiparticle final state more than just one pair of particles may interact strongly. A typical reaction is shown in Fig. 1, in which a pion is produced in pion-nucleon scattering. In the final state $\pi\pi N$, there is the possibility of three interactions: the two πN ones, and the $\pi\pi$. Figure 2 shows a rescattering term representing the production of a pion and a (3,3) nucleon isobar, the isobar then decaying and its decay pion rescattering from the pion. We call the amplitude for this process F. The problem is to calculate F as a function either of the incoming energy W or of the mass of the two pions $\sqrt{s}$.[2]

Graphs similar to Fig. 2 have been discussed quite extensively.[3] Whereas single-particle exchange graphs lead to poles, these give logarithmic singularities—often called anomalous thresholds—in W or s, and some effort has gone into seeing if these singularities lead to observ-

* Work performed under the auspices of the U. S. Atomic Energy Commission.
† Present address: Service de Physique Theorique, C.E.N., Saclay, France.
[1] See, for example, F. Zachariasen, Phys. Rev. Letters **7**, 112, 268 (1961); G. F. Chew, Phys. Rev. **129**, 2363 (1963); and L. A. P. Balazs, *ibid.* **128**, 1939 (1962).

[2] I am indebted to Dr. S. F. Tuan for stimulating my interest in this type of graph. I have been informed by Dr. Tuan that a calculation, similar to that reported here, has been done by Dr. T. T. Wu and himself.

[3] For example, by V. N. Gribov, Zh. Eksperim. i Teor. Fiz. **41**, 1221 (1961) [English transl.: Soviet Phys.—JETP **14**, 871 (1962)], for τ decay, and by V. V. Anisovich, A. A. Ansel'm, and V. N. Gribov, Zh. Eksperim. i Teor. Fiz. **42**, 224 (1962) [English transl.: Soviet Phys.—JETP **15**, 159 (1962)], for pion production reactions near threshold.